Nonlinear Optical Spectroscopy of Polymers

Elizabeth Cavicchi†, Jayant Kumar†, Sukant Tripathy*
Departments of Physics† and Chemistry*
University of Lowell, Lowell MA, USA 01854

I. Introduction

In linear optical spectroscopy, atomic and molecular structure is probed by light. The intensity, frequencies, and spectral width observed in the signal output from a sample--whether by reflection, transmission, absorption or scattering--reveal clues of energy transitions, and hence information about the electronic, vibrational, and other motional and structural aspects at the molecular level. Typically, the probing photons induce transitions between energy levels characteristic of the sample's molecules. Through analysis of the spectral output, the relative pattern of molecular levels can be reconstructed. Nonlinear optical spectroscopy on the other hand, rather than acting just as a probe, strongly perturbs the system. The strong optical electronic fields reorient the molecule's spatial positions, distort electron clouds, and excite uncharacteristic or forbidden transitions. As a result of these processes, the medium's optical behavior becomes field dependent. New optical phenomena have been discovered through these interactions, which may provide evidence of underlying molecular properties not revealed by linear spectroscopy.

An important aspect of current investigations of nonlinear optical phenomena is the development of materials with enhanced nonlinearities and of efficient processing methods. Certain organic and polymeric substances exhibit some of the most pronounced nonlinear responses known. Thus, the interest in nonlinear spectroscopy of polymers originates, not only in the traditional spectroscopic studies of relating macroscopic optical properties to microscopic interactions and structure, but also in the effort to design systems with augmented nonlinear effects which may find application in optical devices or components (1, 2).

This article reviews many of the experimental techniques currently in practice for

detecting nonlinear optical signatures from polymeric samples, their physical basis, and molecular and structural properties which have been inferred from them.

II. Background

The separation of negative and positive charges in a medium under the influence of an applied electric field induces a polarization in the bulk sample whose direction alternates with oscillations in the applied field. The sample's induced polarization, P, can be detected macroscopically by its index of refraction and absorption. For weak applied fields--whether propagating or not--the electric vector, E, induces a polarization, P, in the material with a linear dependence on the applied field: $P_{linear}=\chi^{(1)}E$, where $\chi^{(1)}$ is the three dimensional susceptibility tensor. The resultant polarization in a medium subjected to multiple fields is a linear superposition of the effects caused by the same fields acting independently.

However, at the high intensities available with lasers, optical fields can interact with each other through higher order terms in the polarization vector : $P=\chi^{(1)}E+\chi^{(2)}E\cdot E+\chi^{(3)}E\cdot E\cdot E+...$ $=P_{linear} + P_{nonlinear}$. The applied fields perturb the charge distribution in the medium, in such a way as to alter the behavior of the medium. The nonlinear susceptibilities $\chi^{(2)}, \chi^{(3)}...$, which represent the magnitudes of higher order interactions between the applied fields, are dictated by features at the molecular level including electronic and molecular structure and overall molecular packing. While P is a macroscopic measure of the dipole moment averaged over the volume of the sample, on a molecular scale the dipole moment can be expressed in an analogous fashion as: $p_i=\alpha_{ij}E_j+\beta_{ijk}E_jE_k+\gamma_{ijkl}E_jE_kE_l$. The coefficients $\beta_{ijk}, \gamma_{ijkl}$ are termed the *molecular hyperpolarizabilities.* A detailed analysis of the hyperpolarizabilities in a variety of organic liquids is presented in a paper by Levine and Bethea (3).

This section will sketch mechanisms by which a range of optical effects are produced by the second and third order ($\chi^{(2)}$ and $\chi^{(3)}$) contributions to the polarization vector. The nonlinear optical processes are of interest from two perspectives. The first consists of the traditional province of spectroscopy involving the investigation of interactions between light and materials. Secondly, an understanding of the underlying processes responsible for nonlinear phenomena is sought. This can become the groundwork for engineering materials for technological applications, such as in optical switching. In this view, the goal of nonlinear polymer spectroscopy is not only to observe and describe the polymers' optical behavior, but also to

optimize the magnitude of that response. This, along with related studies, helps to develop approaches to the practical utilization of these materials in optical devices and related technologies.

Optical effects induced by even terms of the expansion of the polarization vector P can be observed only in materials lacking a center of symmetry. The physical properties of a member of a centro-symmetric crystal class must remain invariant to reflections through the crystal's center of symmetry. When a field E is applied to the crystal, the second order polarization term will be $P_{nonlinear}=\chi^{(2)}E\cdot E$. If the coordinate system used to describe the crystal is now inverted, the electric field vector E will be transposed to -E. The polarization vector will change sign to reflect the inversion of the coordinates. However, by squaring the electric field vector (or its inverse), even order terms in the polarization expansion: $E\cdot E$, $E\cdot E\cdot E\cdot E$, . . . yield the same value in either case (E E=(-E)(-E)). This implies that all the even polarization coefficients $\chi^{(2)}, \chi^{(4)}$,... are identically 0 if P is to change sign under inversion. This requirement rules out second and higher even order phenomena in centrosymmetric crystalline materials (11 of the 32 crystal point groups are centrosymmetric), however third and higher odd-order phenomena are still present.

Optical Harmonics

For a linear optical medium, light transmitted through the sample is at the same frequency as the incident light. However, optical nonlinearities in the medium can make the applied fields interact, creating a spectrum of new combinations: harmonics (doubling, tripling, etc.), as well as sum and difference frequencies. Each nonlinear term successively couples the total incident field $E=\Sigma E_n e^{i(k_n\cdot r-\omega_n t)}$ to itself ($E\cdot E$, $E\cdot E\cdot E$, ...). Thus in general, each higher order interaction generates an increasingly diverse array of frequencies: at second order, $2\omega_1$, $2\omega_2$, $\omega_1+\omega_2$, $\omega_1-\omega_2$ ... at third order, the preceding and $3\omega_1$, $3\omega_2$, $2\omega_1+\omega_2$, $\omega_1+2\omega_2$, $2\omega_1-\omega_2$... and so on (4, 5). While the diverse combination frequencies generated from specified input frequencies manifest an intriguing physical phenomenon, these properties can also be exploited in the design of practical devices.

Phase Matching

The power output in the higher harmonic frequency depends on maintaining the relative phases between the incident and radiated waves, as they interact at each point in the medium. When the incident and radiated waves have the same frequency they [illegible]

same velocity. Nonlinear interactions can produce higher harmonics which, because of dispersion, travel at different phase velocities from the fundamental. The output wave at one point may not arrive at another site in phase with the output waves at that site. These waves may interfere destructively before they can depart the sample and be detected. The phase mismatch, Δk, between the fundamental and the harmonic wave vectors gives a periodic variation in the harmonic wave's intensity inside the material. This periodicity, also termed *coherence length*, is expressed by $L_{coh}=(\pi/\Delta k)$. (This differs from the definition of coherence length commonly used in interferometry.) If $\Delta k=0$, the coherence length is infinite and there is no periodic exchange of energy between the fundamental and harmonic beams in the material.

If Δk can be made to vanish, the entire sample--as opposed to one coherence length--can contribute towards harmonic generation. Often this can be achieved by exploiting thermal or rotational dependence of a material's natural birefringence. This enables the fundamental and the output waves to travel with the same velocity. If the velocities of three interacting waves (ω_1,k_1), (ω_2,k_2) and (ω_3, k_3) can be matched in the medium such that wave vector, k_3 of the output wave satisfies $k_3=k_2+k_1$, that is *phase matched* and $\Delta k=0$, than the entire sample will contribute to the output signal. This operation of phase matching typically favors only one of the possible wave vectors, funnelling most of the output power into it. This enables the generation of an output wave at a selected frequency and wave vector (6).

Maker Fringe Technique

The nonlinear optical coefficients of a sample can be measured by a method due to Maker et al. (7, 8). Rotation of the sample gives rise to interference fringes due to the difference in the index of refraction for the fundamental frequency and the higher harmonic. The rotation axis is perpendicular to the propagation direction of the laser beam. The coherence length, L_{coh}, is related to the directionally dependent indices of refraction for fundamental and harmonic waves. By rotating the sample, its coherence length can be periodically altered, bringing optical signals into interference with each other in traversing a sample many coherence lengths thick. Similar effects can be induced in a wedge shaped sample by translation along a direction perpendicular to the beam. In this geometry, variation in the optical path length (by movement of the wedge) induces a periodic variation in the intensity of the higher harmonic wave.

A relative measure of the sample's second order susceptibility, $\chi^{(2)}$ can be obtained from the Maker fringe technique if a reference crystal such as quartz is used to calibrate the

The articles by Kurtz (9), and Jerphagnon and Kurtz (10) provide an introduction to this technique. The ratio of the intensity of the second harmonic generated in the sample to that in a known reference material, which can be directly measured, is:

$$\frac{I_s}{I_r} = \frac{[e_{2\omega}\cdot\chi^{(2)}{}_s :e_\omega e_\omega]^2 (n_r(\omega))^2 (n_r(2\omega))\ \sin^2(\Delta k_s L_s/2)\ (\Delta k_r/2)^2}{[e_{2\omega}\cdot\chi^{(2)}{}_r :e_\omega e_\omega]^2 (n_s(\omega))^2 (n_s(2\omega))\ \sin^2(\Delta k_r L_r/2)\ (\Delta k_s/2)^2}$$

For the sample and reference material, the refractive indices are n_s and n_r and the thicknesses are L_s and L_r. The unit vectors along the direction of the electric field in the fundamental and second harmonic beam are e_ω and $e_{2\omega}$. The phase mismatch between these two beams, as found by the Maker fringe technique, is represented by Δk_s and Δk_r (11). Similar techniques can be employed to evaluate the third order nonlinear susceptibilities in a material using third harmonic generation (12, 13).

DC Effects

The evidence of nonlinear optical interactions in a medium was first demonstrated in the presence of dc fields, in experiments predating the invention of the laser by almost a century (14, 15). A dc or low frequency field E in a sample can introduce birefringence as a result of the distortion of the charge cloud of constituent molecules, or even induce adjustments in nuclear positions. For short optical pulses, the medium's primary response is through electronic readjustments as the massive nuclei cannot adapt to such rapidly changing fields. For a nonlinear medium the series expansion of the macroscopic polarization can be expressed in general as:

$$P_i(\omega)=\chi^{(1)}{}_{ij}(\omega)E_j(\omega)+\chi^{(2)}{}_{ijk}(\omega,\omega_1,\omega_2)E_j(\omega_1)E_k(\omega_2)+\chi^{(3)}{}_{ijkl}(\omega,\omega_1,\omega_2,\omega_3)$$
$$E_j(\omega_1)E_k(\omega_2)E_l(\omega_3)+\ldots$$

where the applied fields are at frequencies $\omega_1, \omega_2, \omega_3$ and the probing optical field is at frequency ω. As the magnitude of the applied field is increased, contributions to P from the second and third order components become appreciable altering the complex refractive index of the medium. The first two terms in the expansion representing this index change:

$$|\Delta n_{ij}|=(1/2)|n_{ij}|^3 r_{ijk}E_k+(1/2)|n_{ij}|^3 p_{ijkk}E_k{}^2\ldots$$

are responsible for the Pockels and Kerr effects, respectively. Since the Pockels or linear electro-optic coefficient r_{ijk} is related to the second order susceptibility $\chi^{(2)}{}_{ijk}$, this term is absent in materials possessing a center of symmetry. However, there are no symmetry restrictions on the term which is quadratic in the applied field. Effects due to the Kerr

coefficient p_{ijkl}, related to the third order susceptibility $\chi^{(3)}_{ijkl}$, are present in all materials.

Optical Kerr Effect

When a medium responds to an applied field in its linear regime, it can be modelled as a set of harmonic oscillators forced by the applied field. The intrinsic anharmonicity of these oscillators becomes apparent under the influence of the intense field of a laser beam as well as applied dc and low frequency electric fields. The nature of this anharmonic response is specific to the electronic structure and molecular arrangements in the material. Even in an isotropic medium, an intense light beam can introduce distortions in the electron cloud causing a birefringence whose persistence is dictated by the response time of the medium. While the response and decay of distortions to the electron cloud occur on timescales comparable to the frequency of the optical radiation, physical realignment of molecules is a much slower process. These two mechanisms of optical response, occurring at disparate timescales, can be separated and probed independently.

Optical Kerr effect was first detected by Mayer and Gires and Maker et al. (16, 17). The oscillating field, E, of an optical beam, in a manner similar to the static dc or low frequency fields, can induce anharmonic distortions in the medium which affect the refractive index. The nonlinear index of refraction n in such a case can be represented as $n=n_o+(2\pi\chi^{(3)}|E|^2/n_o^2)=n_o+n_2I$ where I is the intensity of the optical beam. The refractive index at low intensity is given by n_o, $\chi^{(3)}$ contains components of the susceptibility tensor, and $n_2=(16\chi^{(3)}/\pi^2cn_o^2)$ with c as the speed of light.

III. Nonlinear Spectroscopy

This section sketches the processes underlying some of the spectroscopic techniques routinely used in investigating the nonlinear optical behavior of polymers. Spectroscopic experiments provide a direct record of a medium's response to light, and indirect evidence of the system's intrinsic quantum levels. In linear spectroscopy, many transitions between energy levels are forbidden due to symmetry consideration. However, in the presence of strong applied fields some of these forbidden transitions may occur due to multiphoton absorption. By probing the character of virtual transitions, nonlinear spectroscopy offers unique access to the material's quantum structure, as well as providing information about its bulk susceptibility coefficients $\chi^{(n)}$... . Study of the material's behavior at resonance, or real transitions provides a

complementary view of the intricacies of its quantum structure.

The nonlinear processes discussed in the preceding section give rise to a number of effects such as second and third harmonic generation, sum and difference frequency generation, dc and optical Kerr effects, and linear electro-optic effect, among others. These effects can be effectively utilized to perform spectroscopic measurements of higher order susceptibilities and hyperpolarizabilities by methods such as Raman scattering, degenerate four wave mixing and pump-probe techniques etc. These spectroscopic methods are briefly discussed in the next sections.

Raman Scattering

A single photon, incident upon a molecule in a sample, can interact with it in an elastic or inelastic manner, possibly altering the final state of both. If the energy of the scattered photon remains unaltered and there is only a change in the wavevector, the process is referred to as Raleigh scattering. The photon in this case has been scattered elastically. Occasionally, however, the molecule will redistribute the photon's energy among its vibrational states. The quanta of vibration is termed a *phonon.* A molecular system can be characterized by a number of vibrational states and their associated phonons which may be accessed indirectly through such energy redistribution processes. The information about a molecule's vibrational state obtained by this method complements that available through infrared spectroscopy. The re-emitted photon in such inelastic processes, termed *spontaneous Raman scattering*, differs from the incident photon by the energy excess or deficiency between the molecule's initial and final state. If the molecule's final state is above its initial state, the emitted photon will be downshifted in frequency ($\omega_2 < \omega_1$): a *Stokes* line will be observed in the scattered light as illustrated in Figure 1. An *anti-Stokes*, up-shifted line ($\omega_2 > \omega_1$) is evidence of a molecular transition down from an initial elevated state (18). As the number of pump photons is increased, the presence of Stokes or anti-Stokes photons, created through spontaneous Raman scattering will stimulate further Stokes or anti-Stokes photons by interacting with the excited molecules. This process of *stimulated Raman scattering* gives rise to the same Raman shifts as spontaneous Raman scattering. The output intensity, however, depends exponentially on the pump laser intensity if no pump depletion occurs (19).

The occurrence of Raman-induced jumps between molecular vibronic states alters internuclear distances in the molecule, effecting a

fields drive individual oscillators at their resonant vibrational frequency ω_v. The molecules vibrate at the characteristic vibration frequencies ω_v which modulates the polarizability and hyperpolarizability coefficients of the molecule (α, β and γ). These modulated coefficients can be expanded as, $\alpha=\alpha_1+\alpha_2\cos\omega_v t$, $\beta=\beta_1+\beta_2\cos\omega_v t$, and $\gamma=\gamma_1+\gamma_2\cos\omega_v t$. Upon substitution in the dipole equation, $\mathbf{p}=\alpha\mathbf{E}+\beta\mathbf{E}\cdot\mathbf{E}+\gamma\mathbf{E}\cdot\mathbf{E}\cdot\mathbf{E}$. . . they produce a host of output frequencies, including a Raleigh scattering term at ω, second and higher-order harmonics at $n\omega$, Stokes and anti-Stokes lines at $\omega\pm\omega_v$, and higher-order combinations $\omega\pm m\omega_v$. The distinction between Raman scattering, and parametric generation of harmonics or sum and difference frequencies is that the frequency (ω_v) is intrinsic to the medium and not externally supplied. The new frequencies created by Raman scattering may pump the medium in succession, providing an additional source of higher order lines.

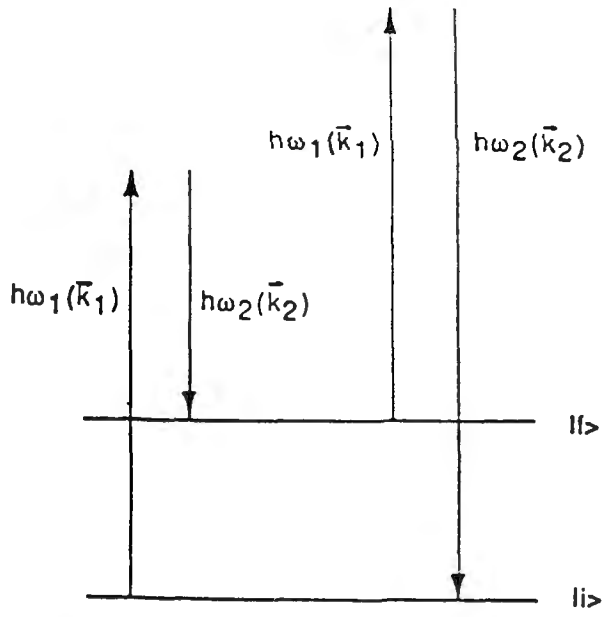

Figure 1. Schematic drawing showing the Stokes ($\omega_2<\omega_1$) Raman transition from the initial state $|i\rangle$ to a final excited state $|f\rangle$, and the anti-Stokes ($\omega_2>\omega_1$) Raman transition from $|f\rangle$ to $|i\rangle$.

If the pump field is strong enough, the oscillators can be driven synchronously, and coherent Stokes and anti-Stokes radiation can be emitted. The acronyms CARS *(Coherent Anti-Stokes Raman Scattering)* and CSRS *(Coherent Stokes Raman Scattering)* denote this type of emission (20, 21). Enhancements in the Raman scattering signals have also been induced through amplifications in the internal fields created at interfaces. In this *Surface Enhanced Raman*

Scattering (SERS) process, internal fields are significantly amplified by appropriate methods of surface preparation (22,23). By this method, Raman scattering experiments have been performed on organic molecules adsorbed or deposited on metalized surfaces.

Stimulated Raman scattering involves only one pump beam. This is a special case of the more general phenomenon of four wave mixing where three different input frequencies may be employed, giving rise to a fourth beam. All these processes are mediated by the third order nonlinear susceptibilities of the medium. The CSRS and CARS are also special cases of this more general four wave mixing process where two input frequencies are involved.

Figure 2 represents one variation of a four-wave mixing experiment, in which three input frequencies, ω_1, ω_2, and ω_3 are employed. A large enhancement of stimulated Raman scattering signal is observed as the virtual levels approach a *resonance* with real molecular levels. The effect of these resonances on the nonlinear susceptibility χ can be expressed as $\chi=\chi_r+\chi_{nr}$, with χ_r due to resonance and χ_{nr} as a non-resonant term. As a resonance is approached, the contribution of χ_r due to that resonance becomes dominant; away from any resonance χ_{nr} is determined by a sum over all the molecular resonances. Thus, the value of χ depends on where in the range of molecular energy levels the molecule is being probed.

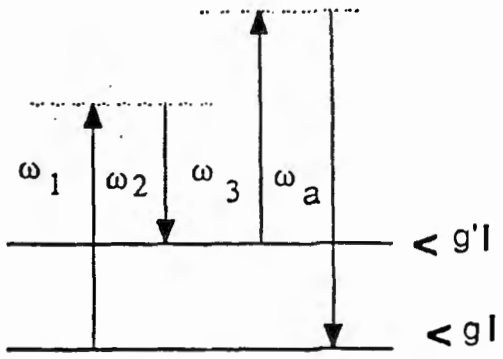

Figure 2. Schematic of a four wave mixing process in which the molecule is elevated from ground state (<gI) to virtual (dotted lines) and real (<g'I) excited states by incident radiation. It finally drops to the ground state with the emission of an anti-Stokes photon. (Reproduced with permission from reference 24.)

Degenerate Four-Wave Mixing

Third order nonlinear optical processes in which all participating frequencies are identical are termed *degenerate four-wave mixing*. Degenerate four wave mixing experiments can provide information about a materials' intensity dependent refractive index which is of

importance for optical switching applications. One geometry commonly used for degenerate four-wave mixing is illustrated in Figure 3 and is analogous to holography. Two waves k_1 and k_1' are incident on a material from opposite directions, while a third, k_i, makes an angle θ with k_1; all three are coherent. The beams k_1 and k_i intersecting at an angle θ interfere, giving rise to an intensity grating in the material, which, in turn, locally modifies its index of refraction, n, through the intensity dependence of n. The result is a diffraction grating created by the material's nonlinear response to the optical field strength as it varies from point to point (25, 26).

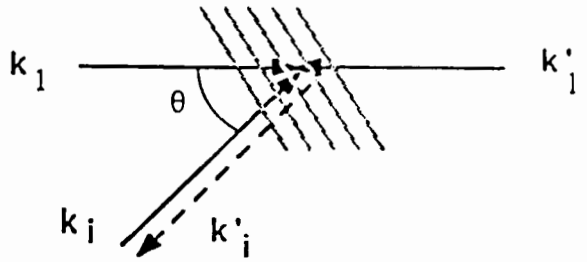

Figure 3. Degenerate four-wave mixing between four waves, all at the same frequency. The output wave, refracted by the grating, is represented by the dotted line.

The modulation depth of the grating, a measure of its deviation from the ambient index of refraction, depends on the relative intensities of k_1 and k_i. The portion of the wave k_i', diffracted by the grating in passing through the material, emerges at angle θ. Although in the general case the three incident waves interfere, forming three gratings within the material, proper selection of the polarization of the waves can result in the formation of only one grating. In the simple case in which one grating is formed within the sample, the third order susceptibility $\chi^{(3)}$ can be determined in a straightforward manner. The ratio of the intensity of the diffracted beam to the pump beam intensity gives the diffraction efficiency of the grating: $I_{output}/I_{pump}=\eta=\sin^2(\pi \Delta n\, L/(\lambda\cos\theta/2))$. Here, L is the thickness of the sample and λ is the wavelength of light. The nonlinear susceptibility $\chi^{(3)}$ can be calculated from the change in index of refraction Δn.

Pump Probe Experiments

Pump-probe experiments, as diagramed in Figure 4, facilitate temporal and spectral analysis of the excited states of the molecule. Radiant energy from a pump beam k_1 excites molecular transitions from the ground state to higher real or virtual states, changing their relative populations and perhaps even the positions of the energy levels. A weak probe beam k_i,

incident on the sample, is monitored for loss or gain in its output intensity. By employing pump and probe beams of picosecond or subpicosecond pulse widths, temporal features of a molecule's very short lived states may be investigated. If a variable time delay is introduced between the pump and the probe pulses, the relaxation behavior of the excited states can be monitored in time.

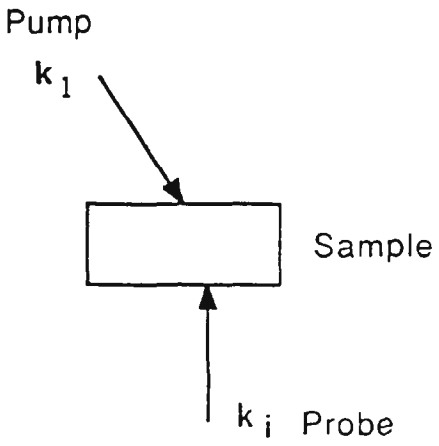

Figure 4. Schematic of a pump-probe experiment. The sample, excited by the pump beam at one time, is interrogated by the probe beam a short time later.

In Figure 5 the temporal sequence of the response of a material to a pump pulse is schematically represented as the probe pulse is delayed in time. By probing at different intervals following the pump pulse, a relaxation curve can be obtained. By tuning the probe wavelength, time resolved spectroscopy of the medium can be performed. This technique can be combined with degenerate four-wave mixing to analyze the relaxation time of the interference grating induced in the medium. The counterpropagating beam may act as the probe--its emission is delayed from the other pump beams.

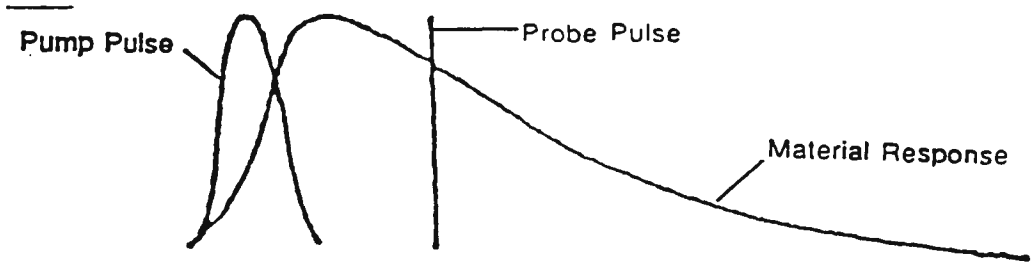

Figure 5. Depiction of the relative durations of pump and probe pulses compared to the material's response curve, in a typical pump-probe experiment. The probe pulse width in this instance is much shorter than that of the pump. (Reproduced with permission from reference 27.)

IV. Polymeric Nonlinear Optical Materials

The early studies in nonlinear optics were performed on inorganic materials which readily fulfilled the standards of superior optical quality--transparency, uniformity, and polished surfaces--that are a minimal prerequisite for any optical work. If the linear optical behavior of the material is well understood and losses incurred by scattering and absorption are minimized, the nonlinear optical effects which are only perturbative can be unambiguously extracted. From these criteria, quartz, used in Franken's discovery of second harmonics (28), seemed ideal: it is transparent to visible and near infrared frequencies and can be grown into single crystals of exceptional optical quality lacking an inversion symmetry. However, the observed signal was quite faint, due to the absence of phase matching and the characteristically low nonlinearity of quartz. Extensive research expanded the set of materials with known optical nonlinearities. A number of inorganic systems such as lithium niobate, barium titanate, potassium dihydrogen phosphate, gallium arsenide and others have emerged as candidate materials for specific nonlinear applications (29,30).

Table 1
Second order nonlinear optical properties. Some values were obtained from reference 31.

Material	n	ε	$r_{ij} \times 10^{-12}$ m/v	$d_{ij} \times 10^{-12}$ m/v
KDP	1.47	42	$r_{63} = 10.6$	$d_{36} = 0.45$
$LiNbO_3$	2.3	78	$r_{22} = 3.4$	$d_{22} = 2.3$
		32	$r_{33} = 32$	$d_{33} = 40$
MNA (2 Methyl-4 nitroanaline)	1.8	4	$r_{11} \sim 67$	$d_{11} \sim 250$
DAN (4-(N, N, dimethylamino-3-acetamonitrobenzene))	1.71	4		$d_{eff} \simeq 27$

Table 2
Values for non-resonant non-linear index of refraction n_2 for some inorganic and organic materials in the near IR. Some values were obtained from reference 32.

Material	n_o	n_2 (esu) (10^{-11})	Response Time (in seconds)
GaAs <100>	3.20	14.1	$< 10^{-12}$
Si <111>	3.44	8.8	$< 10^{-12}$
CS_2	1.59	1.1	$< 10^{-11}$
Fused Silica	1.458	.0095	$\sim 10^{-14}$
PTS Polydiacetylene	1.88	80.0	$\sim 10^{-14}$
MNA (2 Methyl-4-Nitroaniline)	1.8	25.0	$\sim 10^{-14}$
p. nitroaniline		14.0	$\sim 10^{-14}$

Many organic and polymeric materials, however, are expected to far exceed the specific nonlinear response of these inorganic compounds in a material's transparent regime. In addition they are expected to provide advantages in sample preparation and processing. Table 1 gives the index of refraction, n, dielectric constant, ε, the second harmonic generation coefficient, d, and the electrooptic coefficient, r, for a representative pair of inorganic and organic substances. The second order coefficient d_{ijk}, differs from $\chi^{(2)}_{ijk}$ only by a numerical constant. The notation d_{ij} is a collapsed form, indicating that the order of the applied fields, corresponding to the j and k axes, is immaterial. The electrooptic coefficient, r_{ij}, and the dielectric function ε are key parameters for applications in electrooptic modulators. The combination of a lower dielectric constant (indicating faster response to applied electric fields) and a higher second order coefficient establishes the importance of investigating nonlinear optical behavior in organic materials. The comparison of parameters relevant to third order nonlinearities (index of refraction n, third order index n_2, and response time) are presented in Table 2. Extended chain polymeric system with conjugated backbone electronic structure have been found to possess some of the largest non resonant n_2's.

A Simple Picture for the Origin of Nonlinear Effects in Organic Materials

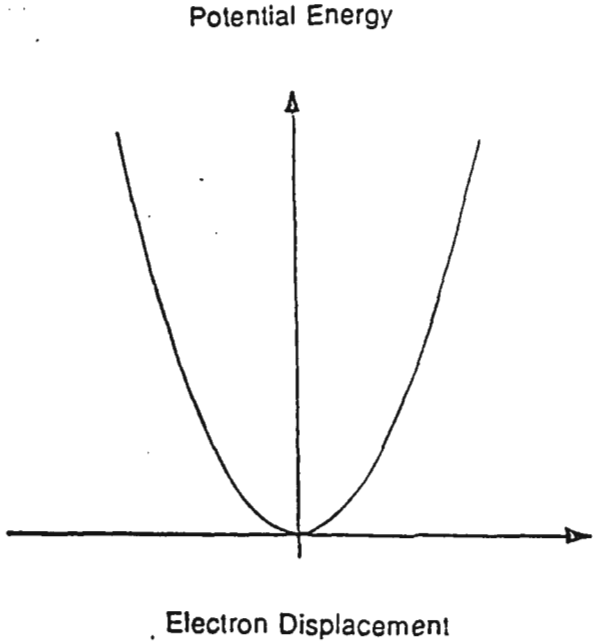

Figure 6. Schematic representation of electronic excursions in a harmonic potential well.

The origin of these nonlinear optical properties is discussed here in the context of a simple intuitive picture. For small perturbations, the response of a valence electron bound to a molecule

may be modelled as a harmonic oscillator. An applied optical field sets these oscillators into forced oscillations. The displacement of a representative valence electron under the collective potential of the rest of the electrons and nuclei in response to an external field is schematically represented in Figure 6. Macroscopically, the collective response of all these oscillators to the imposed optical electric field is observed as the linear index of refraction and optical absorption.

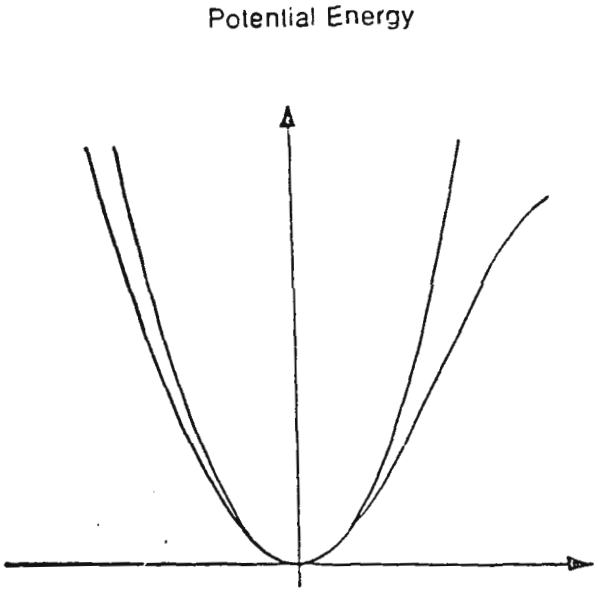

Figure 7. Electronic excursion in an asymmetric anharmonic potential well.

At high applied fields, this harmonic oscillator model breaks down. Electrons, displaced by the field to increasingly larger excursions, "see" significant deviations from the harmonic idealization of the potential (Figure 7). At high applied fields the electronic displacements are significantly larger and electrons experience anharmonic restoring forces. In fact, even when the perturbing fields are relatively small, molecular charge distributions may be manipulated to accentuate anharmonic effects. An asymmetrical distortion of the potential well, for example as

imposed by the addition of electron donor and acceptor substituents to a phenyl ring, could induce such an effect. The presence of conjugation in a molecule--as in the example of the phenyl ring--promotes electronic motion toward the acceptor and away from the donor. Noncentrosymmetric packing of such asymmetric anharmonic oscillators produces large second order effects in the bulk medium. Third- and higher odd-order nonlinear behavior will occur regardless of whether packing in the bulk is centrosymmetric or not.

For a large third- and higher-odd order nonlinear behavior, acentric molecules are not necessary. Third order effects can be modelled by including the fourth order terms in displacement in the potential of an anharmonic oscillator. At high fields, the electrons exhibit significantly larger displacements than would be permitted in a harmonic oscillator well (Figure 8). A π-conjugated polymer backbone promotes this mode of behavior. A highly charge correlated π-electron state leads to a collaborative response of the π electrons to the imposed electric field. Even though the individual valence electrons undergo small displacement the collective response may lead to large nonlinearities. Experimental studies broadly confirm these schematic outlines: systems in which moieties, providing charge asymmetry in low-lying excited states, are attached to a conjugated stem can exhibit pronounced second order effects (provided that the inversion symmetry is broken). Prominent third order effects are associated with polymers possessing conjugated π-electron states (33).

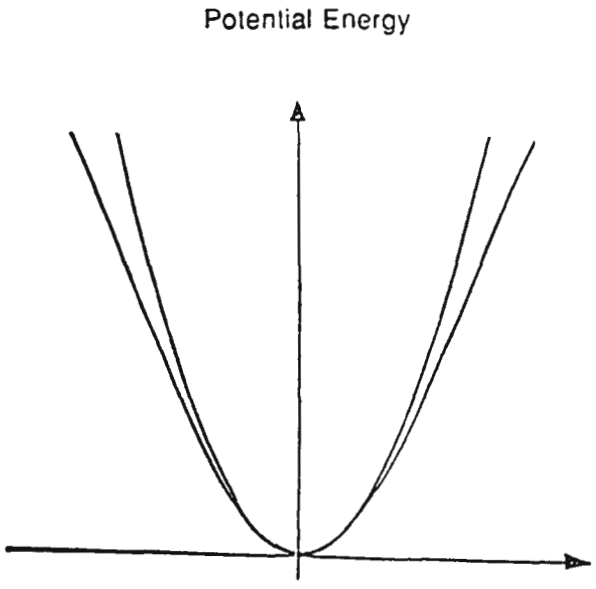

Figure 8. Electronic excursions in a symmetric anharmonic potential well

Polymers with Large Second Order Effects

As discussed earlier, noncentrosymmetric arrangement of molecular units with large molecular hyperpolarizabilities is a prerequisite for significant bulk second order optical nonlinearity. Substantial processing and other advantages are obtained if these molecular units are part of a polymeric system. Candidate polymers must contain, as part of either their main or side chain, units with a large second order molecular hyperpolarizability. An alternative approach is the dispersal, without chemical bonding, of molecular units with large hyperpolarizability into a glassy polymer matrix. The application of an electric field during preparation of such a *guest-host* system prevents isotropic orientations of guest molecules that preclude second order behavior.

A number of vinyl polymers have the possibility of packing in noncentrosymmetric geometries. For example, polyvinylidene fluoride in the β phase has the-CF_2- subunits oriented in the same direction. Although the second order hyperpolarizability of each subunit is relatively small, since half the polymer is comprised of such units, this polymer exhibits bulk nonlinearity (34). While polyvinylidene fluoride can be processed into films or fibers, its polycrystalline nature leads to the attenuation of the propagating signals. Scattering losses in the medium diminish the second order signal, impairing the practicality of this, or other similar, materials for nonlinear applications.

In glassy polymers, such as polystyrene, poly-methyl methacrylate, or polycarbonate, losses due to scattering can be minimized. Glassy polymers have been combined with molecules of known large nonlinearities either by mixing (in guest-host materials) or by chemical bonding. In addition, these materials may be processed by techniques compatible with microelectronics fabrication, such as spin coating. A detrimental property of guest host materials is the occurrence of aggregation or phase separation of the active nonlinear compounds from the matrix except at low concentrations (a few percent). By including the active molecules as side chains of a glassy polymer backbone, their number density can be increased, raising the overall bulk nonlinearity.

One example of a prototypical nonlinear molecule used in a variety of such composite polymer preparations is MNA (2-methyl-4-nitroaniline). Two electron donor groups (NH_2 and CH_3) and an acceptor group (NO_2) are attached to the aromatic ring, producing a dipole moment directed across the ring and a large hyperpolarizability β. As shown in Table 1, the

coefficient observed in MNA is greater than that of lithium niobate. A theoretical calculation of the molecular hyperpolarizability β on the basis of the electronic states in PNA (para-nitroaniline), by Lalama and Garito (35) correlated well with experimental determinations of β (36). Their model identified the asymmetrical geometry of the molecule's charge-correlated π-electron states as a primary factor in generating the high value for β.

Polymers with Large Third Order Nonlinearities

Polymeric materials exhibiting pronounced second order behavior may also possess third order nonlinearities, regardless of packing symmetries in the bulk sample. However, the largest third order susceptibilities have been observed in macromolecules with π-conjugation along an extended backbone. In empirical studies of some polymers (e.g. polydiacetylenes), such a third-order response correlates with the presence of long, essentially one-dimensional, conjugated chains, low-lying charge defect states, or strong absorption in the mid-visible range. The nonlinear signal may be enhanced considerably by resonance-related effects.

Large third order nonlinearities have been demonstrated in a variety of conjugated polymers including polyacetylenes, polythiophenes, and polyphenylene vinylenes (37-39). The optical properties of polydiacetylenes (PDA) are the best defined among the conjugated polymer systems currently under investigation. Theoretical studies evaluating the origin of nonlinear behavior in the polydiacetylenes include the work of Karpfen 1980 (40), Sauteret et al. (41), Agrawal et al. (42), Baughman and Chance (43), Lewis and Batchelder (44), Flytzanis et al. (45). Some of the largest nonresonant third order index of refraction, n_2, have been reported from single crystals and thin films of polydiacetylenes.

While polymers typically are obtained in morphologies with chain entanglements, exposure of monomer single crystals of diacetylenes to ultraviolet radiation or heat, can produce a single crystalline arrangement of polymer chains (46) by topochemical polymerization. The long unbranched chains of PDAs form exceptional crystals by this method, and have been carefully characterized by x-ray and electron diffraction (47). Although monomer PDA crystals are transparent, they convert upon polymerization to an intense color with a metallic sheen (48) and their nonlinear optical response increases by three orders of magnitude (41). This demonstrates the connection between the unique optical properties of polydiacetylenes and the extensive conjugation of the PDA backbone.

Molecular Design and Preparation Methods

In addition to their substantial optical nonlinearities, another asset of organic and polymeric materials is the possibility of extensive structural modification. This can be used towards the optimal design of a nonlinear optical polymer for practical application. The intuitive model described earlier might serve as a basis for developing relationships between molecular structure and nonlinear response. The synthesis of new polymeric forms can diversify and supplement the quest for materials optimized for specific mechanical, thermal, and processing properties as well as for their linear and nonlinear optical characteristics.

The substitution of different electron donor and acceptor groups in the polymer sidechains or backbone may modify the material's linear and nonlinear optical behavior. Toward this purpose, Nicoud and Twieg (49) have adapted rules originally derived by Dewar and coworkers (50) to predict the effect of substitutions on the characteristic wavelength of the chromophore dyes. An optimally designed chromophore such as DANS (4-dimethylamino-4'-nitrostilbene), could be incorporated in a polymeric system to enhance its nonlinear optical properties.

A theoretical study by Orchard and Tripathy predicts the effect of modifications of the sidegroup electronic structure of polydiacetylenes on their bulk electronic properties (51). Significant red shifting of the absorption edge is observed as side groups with the possibility of charge conjugation with the backbone are attached. Empirical confirmation of such an interdependence between structure and optical properties has been demonstrated in studies of polydiacetylene derivatives (52). Kumar et al. (53) have synthesized azomethine dye based polymeric systems in an effort to combine the large third order response of a conjugated polymer backbone with side chain substituents possessing prominent second order properties.

The process of tailoring polymers for nonlinear optical applications often puts conflicting requirements on the material properties. A novel structure with a large efficiency in harmonic generation may have a reduced window of transparency or detrimental mechanical properties. The task of combining all the requirements for optical performance and practicality of use in a single material presents many such conflicts, yet it forms the agenda of molecular engineering.

In the engineering of polymers specifically for their nonlinear optical behavior, two aspects are emphasized: the synthesis of new molecular species with enhanced nonlinear optical properties, and the bulk processing of these molecules in crystals, films, fibers, and other desired forms. The molecular segments constituting a sample can be ordered by the imposition of

thermal, mechanical, electric or other appropriate fields, and thermodynamic variables during processing. In addition to affecting optical response, the methods of sample preparation impact on a material's mechanical properties and possible utility in device configurations as well. For eventual application in optical devices such as waveguides, frequency doublers, and switches, the preparation's integrity, resistance to thermal, mechanical and optical damage, and ease of fabrication will determine the commercial viability of a candidate nonlinear material.

Crystalline polymers present interesting optical properties due to their intrinsic anisotropic structures. Only by first growing single crystals of the monomer followed by topochemical polymerization in the solid state has it been possible to grow single crystals of polymers, either in the bulk or as large area thin films. In a method due to Thakur and Meyler (54, 55), the monomer in its liquid phase (either as solution or melt) is inserted between flat substrates. The monomers form thin crystals upon evaporation of the solvent or cooling of the melt and are subsequently polymerized in place by heat or uv radiation. This method is particularly effective at producing crystals with surfaces of good optical quality. However, its applicability is limited to processing small organic compounds, and it does not capitalize upon many of the bulk processing features that polymers afford.

As an alternative to polymer crystals, the optical properties of samples in the form of glassy polymer films, oriented fibers, or monodomain polymer liquid crystals have been investigated. Although scattering losses in these systems may be greater than in a perfect single crystal, these losses are minimal when compared to losses in polycrystalline or other heterogeneous media. The presence of an organizational order in such preparations can have a significant influence on the material's nonlinear optical effects.

Structural and optical property aspects of two substances can be advantageously integrated, for example, by incorporating a molecule such as MNA with nonlinear optical behavior, in a liquid crystal or glassy polymer host. The host, elevated by heating to its nematic or viscous phase, or (for the glassy polymers) beyond its glass transition temperature, may be aligned by the influence of an applied electric field. The guest dipoles, initially oriented randomly, tend to flip to align with the field. Rapid cooling, in the presence of the field, produces a poled sample which retains its orientational integrity (at least partially) in the absence of the field. The electrode configuration may be designed for use both in poling and in subsequent use as part of an electrooptic device. Guest-host structures are introduced in the reviews by Williams (56, 57)

while the articles by Hill et al. (58), Pantelis et al. (59) and Singer (60) discuss current optical research performed with these materials.

The *Langmuir-Blodgett* or *L-B* method offers another way of preparing polymeric samples for nonlinear optical research. Molecules with a polar head and a hydrophobic tail may be organized as a monolayer at the air water interface. These molecules may be designed containing a polymerizable group and in addition groups with large nonlinear optical coefficients. A solution of the surfactive monomer in a volatile solvent is deposited on a water surface. By laterally compressing the film the molecules form a compact phase before the film collapses. The monolayer is transferred as a substrate is mechanically lowered and raised through the surface. If the barrier maintains a constant surface pressure, this process may be repeated for the preparation of multilayer films (61).

The mode of deposition, in part, determines the relative orientation of deposited monolayers; a substrate dipped both in and out typically acquires a Y-type film whose layers alternate in a head-tail-tail-head pattern (Figure 9). Using monolayers of two different molecular species A and B, composite Y-type layers of an ABAB... structure may be deposited. X-type (all polar heads up, Figure 10) and Z-type (heads down, Figure 11) films although noncentrosymmetric are less stable and may revert to the preferred Y-type configuration.

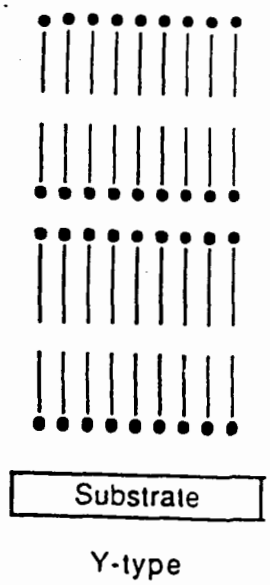

Y-type

Figure 9. Y-type orientation of molecular layers in a Langmuir-Blodgett multilayer film.

The Langmuir-Blodgett method allows precise control in layering complete planes, consistent in thickness and orientation, of organic molecules. X-ray and electron diff...

studies (62, 63) have demonstrated that a degree of crystalline order can be attained in these films. Yet, due to the polycrystalline nature multilayer structures do sustain significant scattering losses. In spite of this problem the above features, combined with the option of incorporating molecules or moieties with substantial optical nonlinearities into the L-B films can be used to investigate device concepts and optical properties in a unique manner.

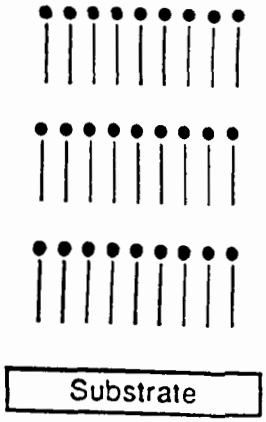

X-type

Figure 10. X-type orientation of molecular layers in a Langmuir-Blodgett multilayer film.

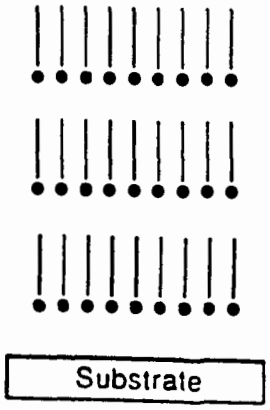

Z-type

Figure 11. Z-type orientation of molecular layers in a Langmuir-Blodgett multilayer film.

Fragile films formed from monomers, such as vinyl stearate or diacetylenic acid, can be stabilized by polymerization subsequent to transfer onto a rigid substrate. Both the thickness and molecular orientation of the film may be controlled through the preparation process. Given the role of inorganic film technology in VLSI circuitry, the prospect of uniform organic films has elicited considerable interest. Among the many reviews of this burgeoning field are those of Swalen (64), Blinov (65), Barraud (66), Rabolt et al. (67), and Kowel et al. (68).

V. Investigations of Nonlinear Phenomena in Polymers

In the following sections several representative experiments will be discussed to illustrate the techniques described earlier to investigate the nonlinear optical properties of polymers. There is a large and rapidly growing body of literature on the nonlinear optical properties of polymers. In this review a number of recent research reports on both second and third order effects in polymers have been discussed. In conjunction with a number of earlier reviews this should provide a comprehensive coverage of nonlinear spectroscopic techniques and their applications to relevant polymeric systems.

Electroreflectance and Electroabsorption Spectroscopy

As discussed earlier external electric fields can perturb the electronic states of an atom or a molecule. Weakly bound electrons are particularly susceptible to perturbation due to external fields. The field binding the valence electrons to the molecules in many molecular systems are not very strong, and field strengths accessible easily in a laboratory (10-100 kV/cm) can appreciably modify the attractive potential between the electrons and the molecule. Electrons weakly bound at a defect site, delocalized along a conjugated polymer backbone or molecular unit, and weakly bound excitons (electron-hole pairs) can be easily perturbed due to applied fields. Excitonic and other charge defect states in several conjugated polymers are not as loosely bound as in some inorganic semiconductors but have dimensions in the range of 20-30 Å. At lower temperatures the absorption spectra due to excitons and other defect states are much sharper due to longer lifetimes and reduced probabilities of rapid vibrational relaxation. Macroscopically, perturbations induced by a field on these electronic states can be observed through Stark effect shifts in the characteristic spectrum of the sample. The spectrum, altered by fields typically of 10-100 kV/cm, may be viewed either in reflection (*electroreflectance*) or in absorption (*electroabsorption*).

Sebastian and Weiser (69-71) have compared reflectance spectra of single crystals of the polydiacetylenes, DCHD (poly1,6-bis-carbazolyl-hexa-2,4-diyne) and PTS (poly 1,6-bis-p-toluene sulfonate-hexa-2,4 diyne) in the presence and absence of external electric fields. Light from a monochromator was incident normal to freshly cleaved faces of crystals cooled to a few degrees Kelvin. By modulating the applied voltage at a fixed frequency and monitoring the modulation in the reflected beam using a lock-in amplifier at twice the modulating frequency, reflectivity changes of 1 part in 10^6 was measured.

The spectra displayed in Figure 12 show the dependence on both the polarization direction of the incident beam, as well as the direction of the external field. Maximum coupling among the DCHD sample's π-electrons oriented along the polymer chain, the optical field, E, and external field, F, occurs when both fields are parallel to the polymer chain direction. This is a consequence of one-dimensional ordering of the conjugated backbones in the polymer crystals, along which π-electrons are delocalized. By contrast, when the electric field is applied along a direction perpendicular to the polymer chains, its influence on the reflectance spectra is three orders of magnitude smaller. Large anisotropic behavior of this kind has not been observed in inorganic semiconductors, which otherwise provide the standard model for describing such phenomena.

The prominent 2.3 eV peak in the electroreflectance spectrum above is interpreted as the band edge. The sample's photoconductivity rises when excited above this energy. Figure 13 illustrates the material's response at this transition point to increases in applied field strength. There is considerable broadening of the peak at stronger applied fields. Using the theoretical analysis of Lochner et al. (72), the authors fitted this broadening to the 2/3 power of the applied field ($F^{2/3}$), which yielded an electronic effective mass $m_e^* = 0.05 m_e$, and a high mobility of 2800 $cm^2/Vsec$ for the electrons. By examining differences between the electroreflectance spectra of DCHD and PTS, Sebastian and Weiser (70) were able to determine the effect of the carbazole side group in DCHD. Strong coupling between the carbazole side group and the π electrons of the polymer chain is evident by the enhancement of photoconductivity at the carbazole's excitation energy of 3.5 eV in the ultraviolet. PTS did not exhibit a comparable response at this energy.

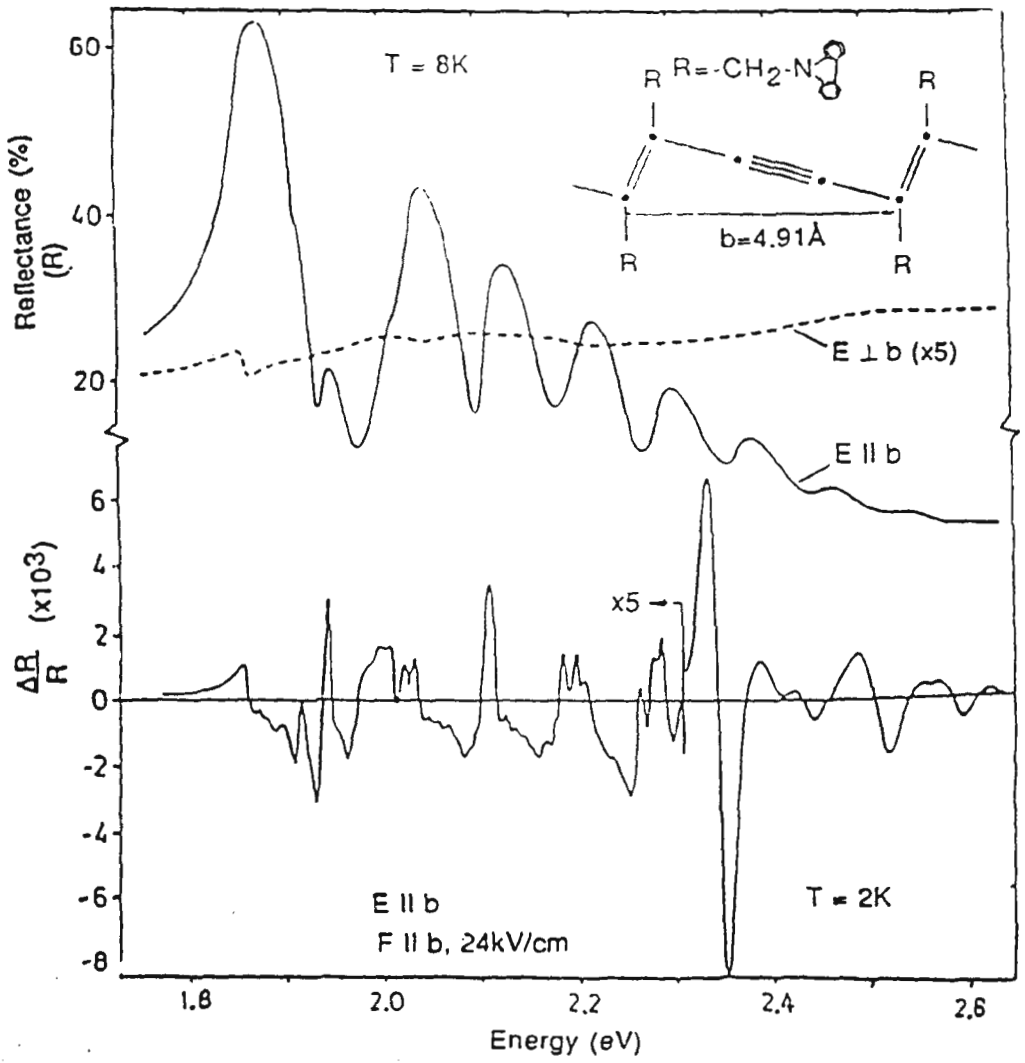

Figure 12. Comparison of reflectance and electroreflectance spectrum for the polydiacetylene (PDA) DCHD. The field is applied at 24 kV/cm at 2 degrees K. (Reproduced with permission from reference 69.)

Tokura et al. (73-75) have investigated the electroreflectance spectrum of polydiacetylenes substituted symmetrically with fluorobenzenes. Figure 14 shows the electroreflectance spectra due to two different excitonic transitions in PDA substituted with 2,5-trifluoro-methyl-benzene (PDA-DFMDP). Only the odd-parity B_u excitons are dipole permitted without a field; when a field is applied, mixing between B_u excitons and even-parity A_g excitons allows both. The principle peak in the ordinary reflectance spectrum is near 2.2 eV. In the electroreflectance spectrum, an additional sharp peak with sidebands appears at 2.8 eV. The authors correlate the first peak with the B_u exciton, and the second peak with the forbidden A_g exciton. The B_u and A_g exciton oscillator strengths calculated as 1.5 and 3.2, respectively,

enabled the authors to compute real and imaginary parts of $\chi^{(3)}$, which exhibited a dependence on the forbidden A_g exciton contribution.

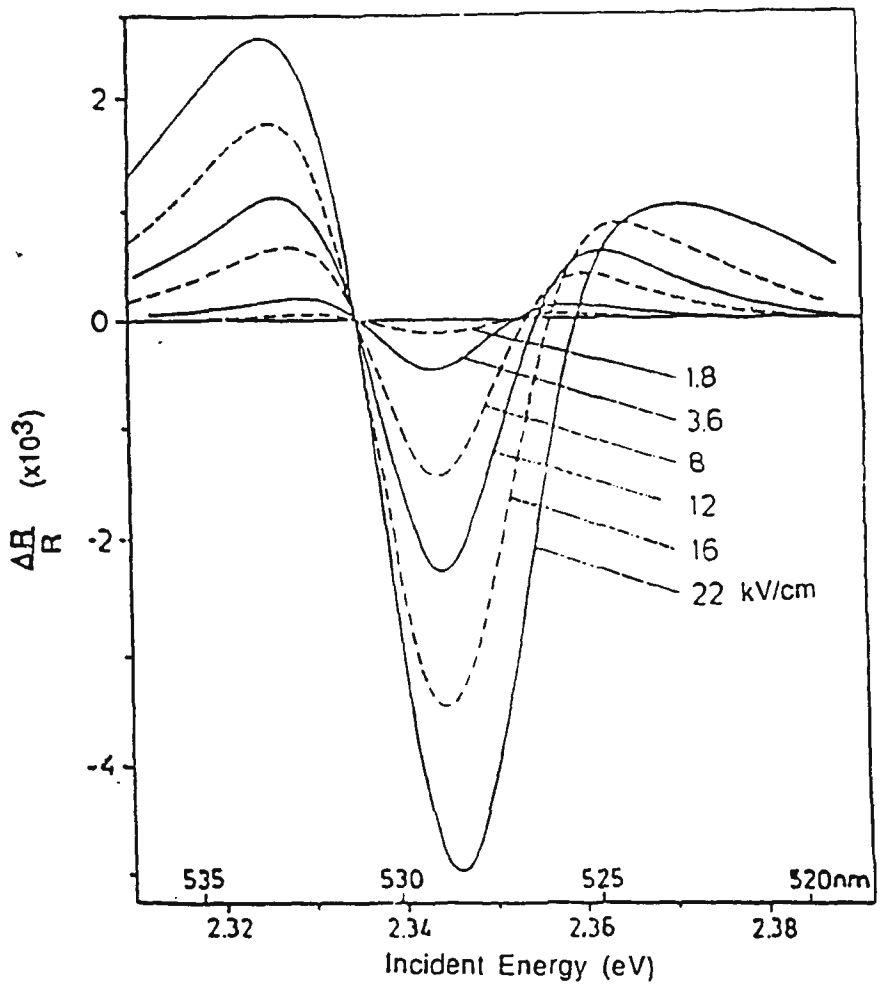

Figure 13. Broadening of the reflectance signal near the band gap with increasing applied electric field. Both applied fields E and F are parallel to the polymer chain axis.

Alterations in the absorption spectrum resulting from the application of an electric field can provide information similar to that obtained by electroreflection. Recently Worland et al. (76) observed electroabsorption in thin films of *trans*-polyacetylene and poly(3-hexylthiophene) subjected to dc fields of 30 kV/cm. The spectral change in transmission, as plotted in Figure 15, is greatest at 1.41 eV, the band edge. Since this absorption change depends quadratically on the applied field strength, it is interpreted as a third order nonlinear effect. The authors determined the real and imaginary parts of the sample's nonlinear susceptibility $\chi^{(3)}$ by applying the Kramers-Kronig relationship. Although this technique is relatively straightforward to implement it is usually applicable only near the material's resonant transitions. Furthermore, it does not provide information about the excited state lifetimes.

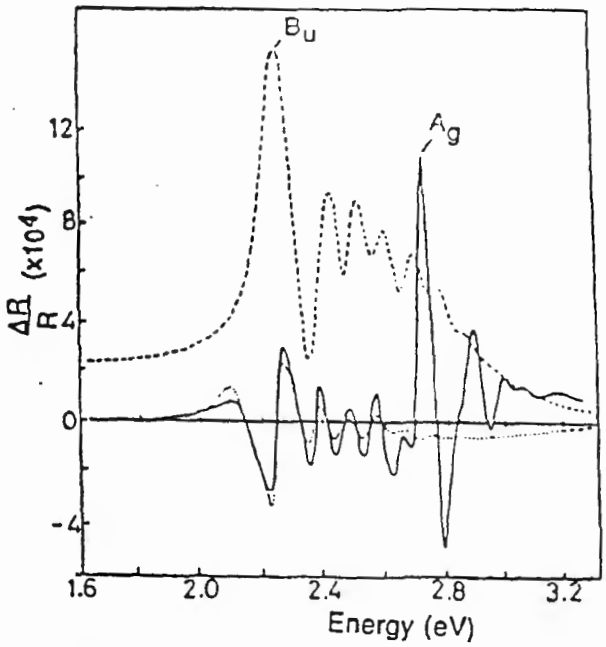

Figure 14. Reflectance (dashed line) and electroreflectance (solid line) spectra in a PDA-DFMDP crystal. Both the external electric field (F=36 kV/cm) and the optical field E are parallel to the chain axis. The dotted line is the energy derivative of the reflectance curve.

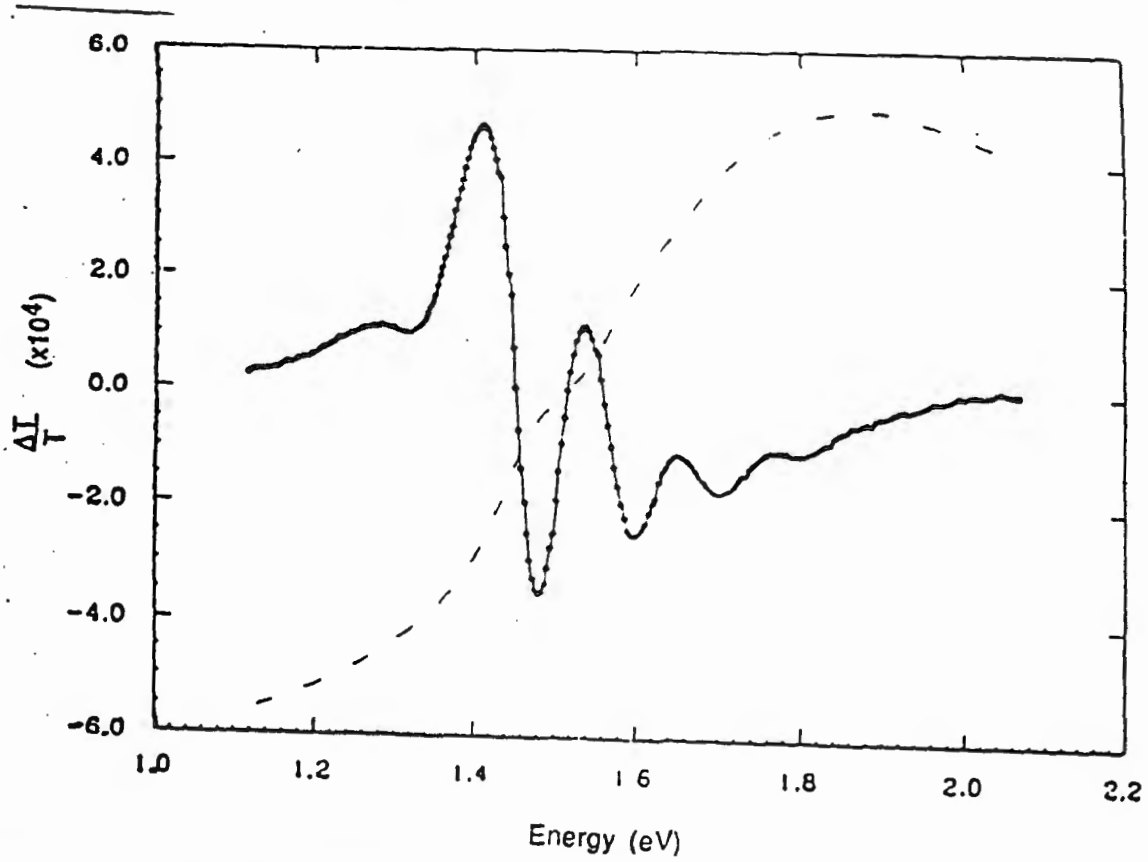

Figure 15. ΔT/T for *trans*-polyacetylene film subjected to a field of 3×10^4 V/cm. The dashed line represents the unperturbed, absorption.

Second Harmonics

While a number of investigations on second order nonlinear optical properties of polymers have been reported, few experiments report spectroscopy of $\chi^{(2)}$ or β. This in part, is due to the difficulty of obtaining intense pulsed tunable laser sources in the near infrared. Contemporary research has remained focussed on the candidate material's optical response at a single input frequency, typically 1.06 micron radiation from a Nd: YAG laser. From a comparison between the intensity of the second harmonic emitted by the sample and by a reference material, values for the effective nonlinear susceptibility $\chi^{(2)}$, the coefficient d_{ijk}, and, indirectly, the hyperpolarizability β may be determined. Second harmonic generation from a number of polymeric systems in various forms are discussed in the following sections.

Second Harmonics from Solutions

Most polymers organize naturally into structures possessing a center of symmetry and ordinarily do not exhibit second harmonics. However, the application of an external dc field breaks this symmetry, and second harmonics, created by the third order polarization term, can be observed. In molecules possessing a center of symmetry, the entire observed second harmonic signal is due to third order effects. Second harmonic signal can arise either due to third order hyperpolarizability, γ, or second order hyperpolarizability, β. In some cases the contributions due to γ and β can be separated out by investigating the time resolved emission of the second harmonic signal.

For dc induced second harmonic generation, the polarization vector along the direction labelled 1 in the laboratory, may be written as

$$P_1^{2\omega}=\Gamma_{1111}E_1^{o}E_1^{\omega}E_1^{\omega}.$$

Here all the applied optical (E^{ω}) and electric fields (E^{o}) are parallel to the 1 direction. Since the intensity of the 2ω line is quadratically dependent on the polarization, it should increase as the square of E^{o} and as square of the incident intensity. The term $\Gamma_{1111}E_1^{o}$ may be considered as an effective second harmonic susceptibility, where

$$\Gamma_{1111}=Nf^{o}(f^{\omega})^2f^{2\omega}[\gamma+(\mu\beta_x/5kT)].$$

In conjugated molecules, the hyperpolarizability, γ, satisfies the relation $\gamma<<(\mu\beta_x/5kT)$ where μ, the ground state dipole moment, is aligned along the molecular x-axis. N is the number density of the molecules, and the f terms are local field factors. The vector component of β_{ijk} is given by

$$\beta_x=\beta_{xxx}+(1/3)(\beta_{xyy}+\beta_{xzz}+\beta_{yyx}+2\beta_{zzx}).$$

Local field effects and solute-solvent interactions, must be taken into account for comparison between experimental values and gas phase theoretical calculations.

An experiment for generating a second harmonic signal in the presence of a dc field, is discussed below. A pump beam from a tunable pulsed laser, directed on a hydrogen gas cell, stimulates a Raman scattering shift in wavelength. This generates a tunable infrared pump beam. A set of prisms are used to select the proper Stokes line and focus it on the sample. Two electrodes apply a pulsed high voltage field to the sample (either a film, solution, or crystal). The second harmonic component of the beam is selected by filters and detected by a photomultiplier, where the signal can be integrated over several pulses and compared with the reference signal.

The sample, typically a solution, is contained in a wedge-shaped cell. By moving the cell along a direction perpendicular to both the direction of beam propagation and the dc field, the optical path length in the solution is changed. The resulting Maker fringe pattern yields a value for the characteristic coherence length. By comparing the second harmonic intensity emitted by the experimental material with that of a reference material, such as quartz, the sample's effective $\chi^{(2)}$ may be calculated. With a tunable light source, the frequency dependence of $\chi^{(2)}$ and β can be analyzed. Teng and Garito have determined the frequency dependence (dispersion) of β_{ijk} in dioxane solutions of PNA and MNA by this method (77,78).

When an electric field applied to a solution is switched off, the orientation of the dipoles of the dissolved molecules is randomized with a characteristic relaxation time. Levine and Bethea (79) observed this relaxation of orientation in solutions of the polypeptide poly-γ-benzyl-L-glutamate (PBLG) following termination of the electric field as a change in the intensity of the second harmonic signal. By delaying the fundamental laser pulse with respect to the applied electric field pulse and measuring the fall off of the second harmonic intensity as shown in Figure 16 they were able to measure β. The decline of the second harmonic intensity, an indication of the solution's relaxation, with increasing delay from the field pulse, is presented in Figure 16. A value of $5 \times 10^{-28} \pm 50\%$ esu for the PBLG's hyperpolarizability β, was determined from this data. While this is a very high value for a molecular hyperpolarizability, it is due to the collective effect of the large number (about 2500) of monomer repeat units which form the polypeptide α-helix. The monomer exhibits a more modest hyperpolarizability of 2×10^{-31} esu.

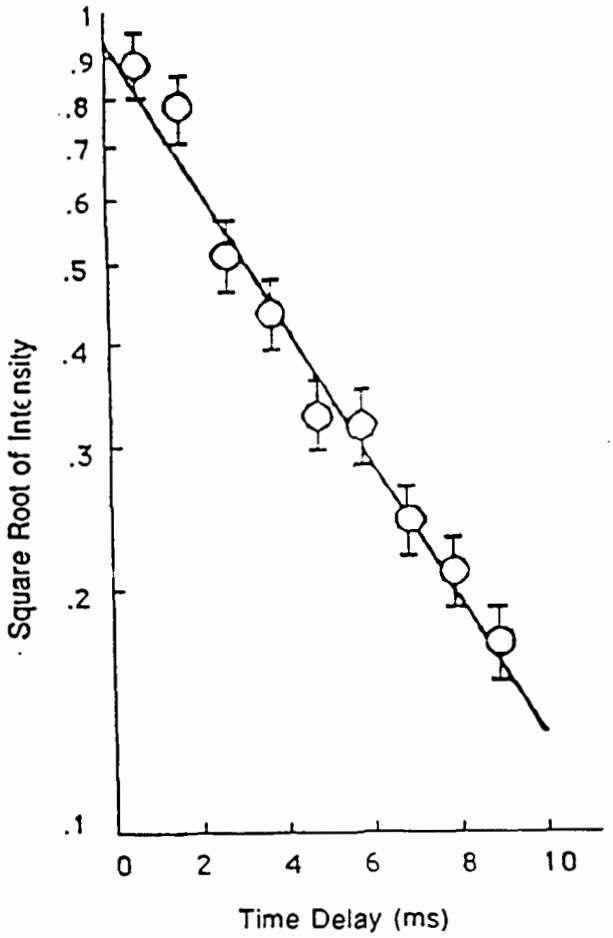

Figure 16. Decrease in the second harmonic intensity as the relative time delay between pulses of the electric field and incident laser beam obtained from a solution of PBLG.

Second Harmonics from L-B films

Monolayer films are intrinsically asymmetric and exhibit second harmonics (80-83); however, when a substrate is repeatedly dipped through the monolayer surface accumulating multilayer films by the L-B method, this asymmetry is not retained. Successive layers tend to orient in a Y-type, head to head or polar end to polar end, configuration, imparting a center of inversion to the film geometry. The second harmonic intensity emitted from L-B samples with even numbers of layers is nearly non-existent (or much less than the monolayer signal), while that from odd number of layers is comparable to the monolayer signal (57, 84-86). The application of a high voltage dc field disrupts this symmetry. Chollet et al. (87) have observed second harmonics emitted from multilayered polydiacetylene L-B films.

From the evidence cited above, multilayering of sample films appears to confer no advantage for generation of second harmonic signals. However, Girling et al. (85,86) and Hayden et al. (88) circumvented this problem by alternately dipping the substrate through merocyanine dye and ω-tricosenoic acid. With the ω-tricosenoic acid layers interleaving the layers a

noncentrosymmetric arrangement of the nonlinear optical material is obtained. This molecular assembly therefore shows significantly larger second harmonic response. Using the same tactic, Kowel et al. (89) have formed active films of hemicyanine dye and hemicyanine-PMMA mixtures. Hayden et al. produced z-type, head-to-tail films (figure 11) from a mixture of hemicyanine dye in either PMMA (88, 90) or poly(octadecyl methacrylate) (91) by depositing layers only on the upstroke of the dipping process. However, they found films composed of alternating inert and active layers exhibited a greater structural uniformity and more consistent optical quality. In these multilayered films, the proportionality constant between the second harmonic intensity and the square of the incident intensity increased with the number of layers.

Berkovic and Shen have monitored variations in the second harmonic signal emitted by monomers floating on water in an LB trough during the polymerization process (80). Laser light, focussed onto the monolayer, excites a second harmonic which is reflected from the surface and passes through a selective filter before the photomultiplier detects it. A second harmonic signal created at the pure water surface could be distinguished from that of the monolayer. Irradiation with uv light (in a nitrogen atmosphere) initiated polymerization in the films. During polymerization, the second harmonic intensity varied continuously from a value characteristic of the monomer to that of the polymer. The intensity observed from monomer films of vinyl stearate and octadecyl methacrylate was higher than from the polymer films. No such change was, however, observed in the diacetylenes. The nonlinearity of the first two monomers is dominated by the π-electrons; polymerization, by breaking these double bonds, diminishes the effect. Since, in diacetylene films, second harmonic emission is unaffected by polymerization, it must arise from an excitation of a segment of the monomer that polymerization does not disrupt. The carboxylic acid end group, which is the only asymmetry on diacetylenes, must be the source of second harmonics, as the diacetylene core, in the monomer and upon polymerization is essentially centrosymmetric. Other studies corroborate this view (92): second harmonics can be observed in diacetylenes only when two different, markedly asymmetric, constituents are bonded to the diacetylene functionality.

In the studies by Chollet et al. (93, 87) second harmonic has been produced in L-B films formed by the transfer of one hundred layers of a cadmium salt of a diacetylenic monomer to a fused silica substrate, followed by polymerization. The films were subjected to tunable laser pulses in the presence of a pulsed applied field (up to 40 kV/cm). The third order susceptibility,

$\chi^{(3)}$, found by comparison with a quartz reference, is plotted as a function of wavelength in Figure 17. The peak at 1.3 μ in the third order susceptibility is a result of resonance enhancement due to two photon excitation.

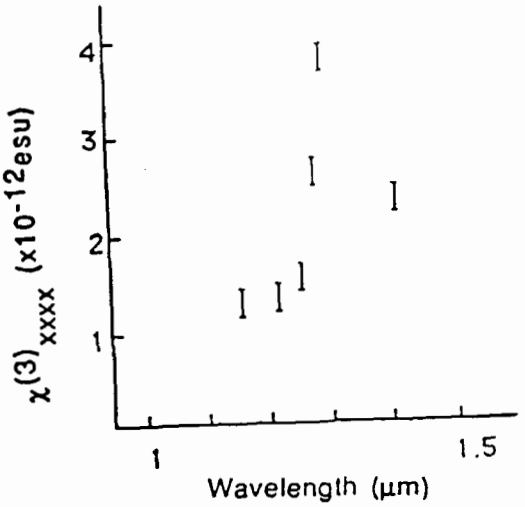

Figure 17. The wavelength dependence of $\chi^{(3)}_{xxxx}$ in LB films of polydiacetylene. (Reproduced with permission from reference 87.)

Bergman et al. (34) were the first to obtain second harmonics from a polymer film. A focussed beam from a Q-switched Nd:YAG laser, with a peak power of 100 W, and commercially available polyvinylidene fluoride (PVF_2) film were used for the experiment. When these films are heated and cooled in the presence of an electric field, the dipoles of the polymer crystallites become fixed in an orientation parallel to the field direction and exhibit pyroelectricity with a mm2 symmetry. Above a threshold poling field of 300 kV/cm and temperature of 100°C the material exhibits pyroelectricity and second order nonlinear effects. When the incident fundamental beam is polarized normal to the plane of the film, the polarization of the resultant second harmonic signal is in the same direction ($E_\omega \| E_{2\omega} \| z$). However, when the fundamental beam was polarized along the plane of the film, the output polarization was perpendicular to it ($E_\omega$not$\| E_{2\omega} \| z$). This observation confirms the assignment of mm2 symmetry. By using the Maker fringe technique, the authors obtained values for the coefficients d_{33} and d_{31} which are of the order of the value for d_{11} in quartz crystals.

Sato et al. (94), by a method similar to that of Bergman, have observed second harmonics in amorphous vinylidene cyanide/vinylacetate copolymer (Poly(VDCN/VAc)) films, which also belong to the mm2 symmetry class. During th...

urs at 180° C in a 500 kV/cm field. On the basis of Maker fringe data, the susceptibility $\chi^{(2)}_{33}$ was determined to be 20% greater than $\chi^{(2)}_{31}$. The quadratic dependence of the second harmonic intensity on that of the incident beam is depicted in Figure 18. In another study of Poly(VDCN-VAc) conducted by Robin et al. (95), the response of the second harmonic intensity to the poling temperature revealed a phase transition at 165° C as shown in Figure 19. An electric field was applied continuously during the poling process. Recently second harmonic signals have been observed in vinylidene fluoride trifluoroethylene copolymers (Poly(VDF-TrFE)) as well (58).

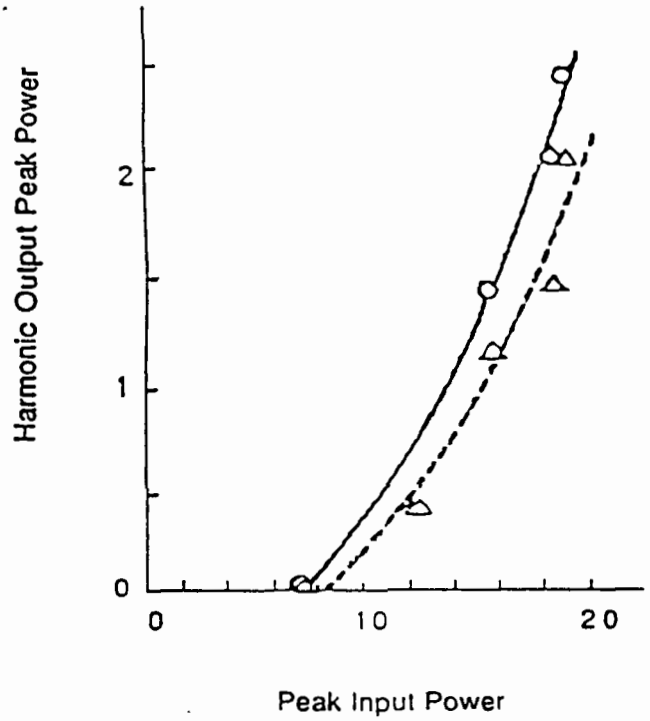

Figure 18. Relationship between the peak power of the second harmonic and the fundamental in P(VDCN/VAc) copolymer films. The incident beam was polarized either parallel to (circles), or perpendicular to (triangles), the direction along which the sample was poled.

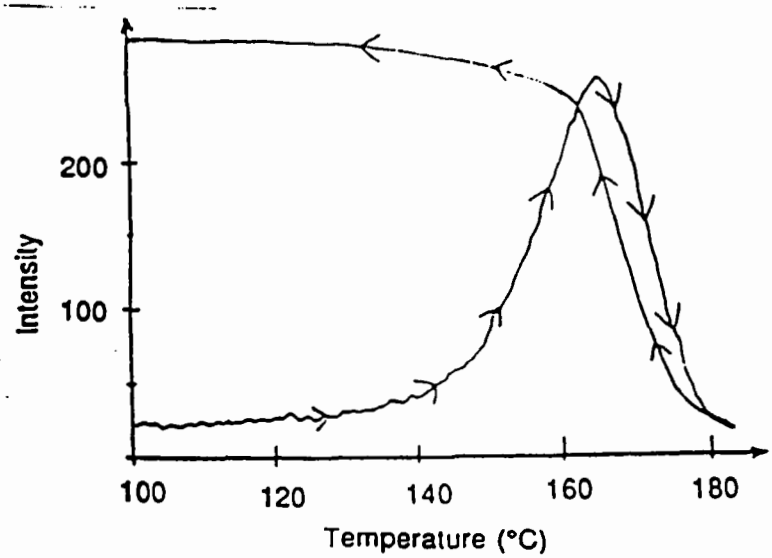

Figure 19. Temperature dependence of the second harmonic intensity in P(VDCN-VAc) films subjected to a continuous electric field.

Guest-host materials, by incorporating the substantial nonlinearities of selected organic molecules (such as DANS) into a polymer matrix characterized by optical clarity and ease of processing, have the potential of exhibiting enhanced nonlinear optical properties. Meredith et al. (96) investigated this behavior in films cast from a liquid crystalline polymer doped with DANS and poled above its glass transition temperature. From the film's optical absorption spectra, the absorbance along directions parallel ($A_{||}$) and perpendicular ($A_{\perp}$) to the applied field were determined. These absorbances define an order parameter:

$$S=(A_{||}-A_{\perp})/(2A_{\perp}+A_{||}),$$

which is a measure of the degree of molecular alignment in the sample (S=1 if all are aligned; 0 if alignment is random). The empirical value of 0.3 for S indicates that the authors' sample experienced a modest degree of alignment following poling. The intensity of the second harmonic emitted by this sample was 100 fold greater than that observed in PMMA poled films doped with the same weight percentage (2%) of DANS. Cooperative interactions between guest and host molecules in the liquid crystalline polymer was suggested as the reason for this enhanced nonlinearity. By comparison with a quartz standard, the susceptibility $\chi^{(2)}_{111}$ was evaluated as $3x10^{-9}$ esu, which is in agreement with a value calculated from a simple "oriented gas" model.

Singer et al. have analyzed second order effects in guest-host materials through both theoretical and experimental studies (97-100). In their experiments, spin coated films of the transparent glassy polymer PMMA doped with Disperse Red 1 dye (4-(N-ethyl-N-(2-hydroxyethyl)) amino-4' nitroazobenzene) are prepared on indium tin oxide (ITO) coated glass substrates. An electric field of (0.2-0.6 MV/cm) was applied to the sample while it was heated above the glass transition (T_g~95^{o}C). The poled sample is noncentrosymmetric; and when excited with laser light at 1.58 μ, a second harmonic signal is emitted. The value of the second order coefficient d_{33} increases nearly linearly with the concentration of the dopant, as plotted in Figure 20. This suggests that the interactions between molecules which depend on the concentration are minimal. The non-zero y-intercept indicates that the PMMA host contributes to the nonlinear susceptibility, perhaps through its poled orientation.

From the purview of spectroscopy, the frequency dependent variation of the second order coefficient is a pertinent quantity. Singer et al. (98) have developed a two-level theoretical model to predict the dispersion curve of d_{33} which is presented in Figure 21. At the shorter

velengths, there is an evident enhancement of d_{33} due to resonant effects. An experimental vestigation of the dispersion of d_{33} would provide a means of evaluating the validity of this model.

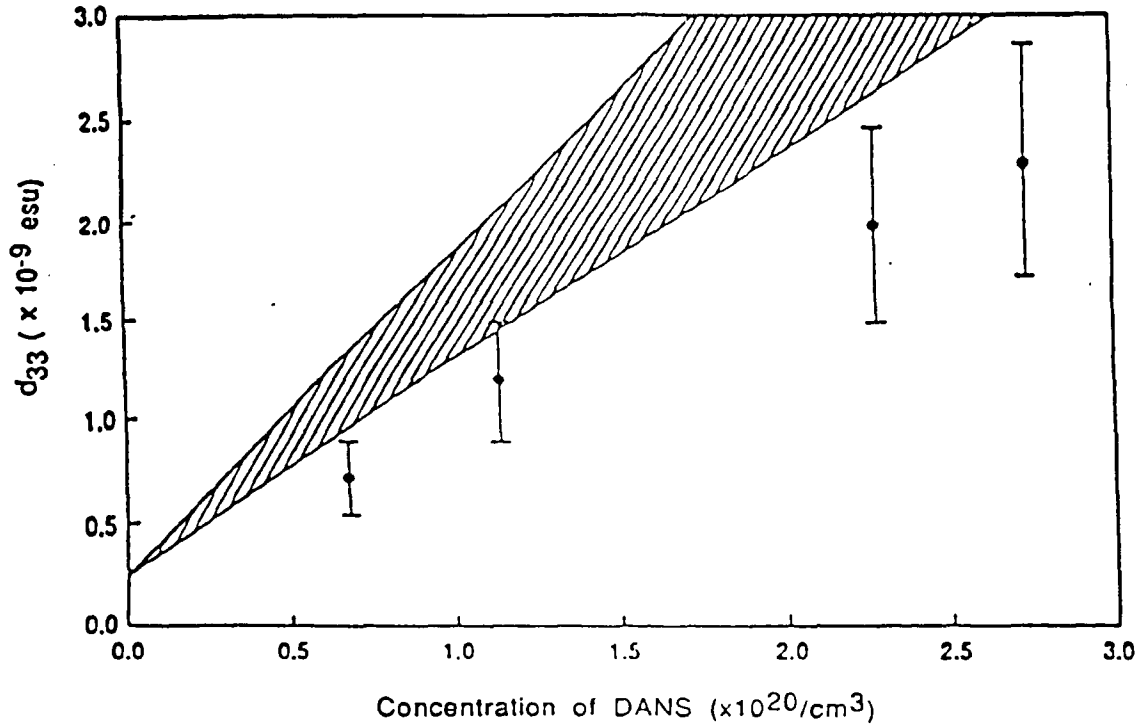

Figure 20. Dependence of the second order coefficient d_{33} on the concentration of the dopant in a guest-host system. The shaded area represents the prediction from a thermodynamic model developed by Singer et al.

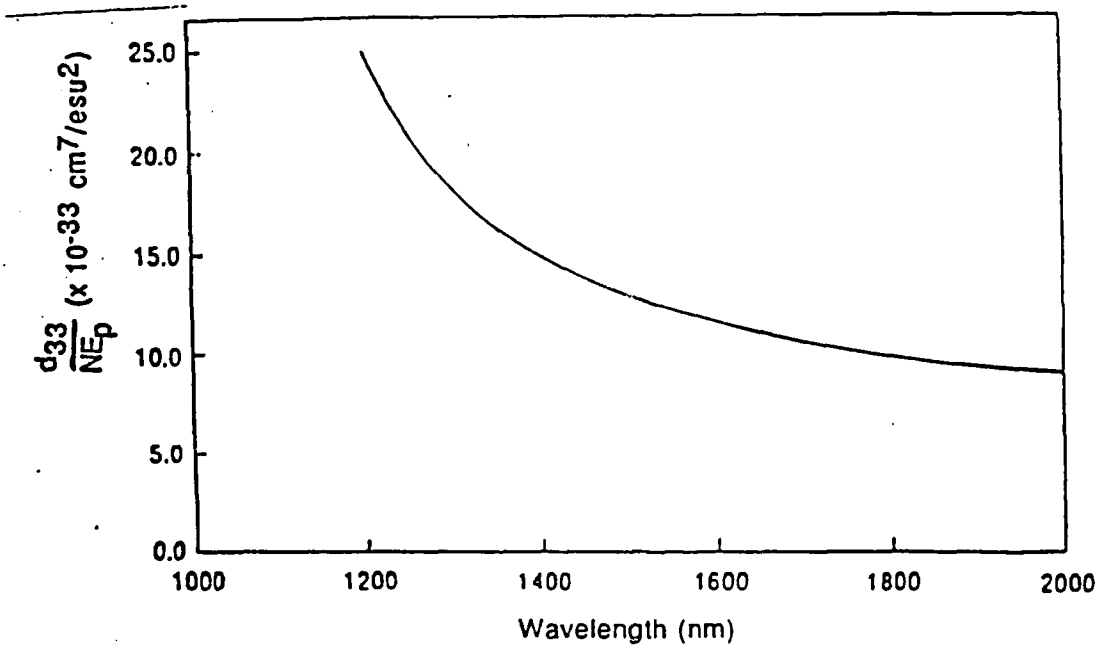

Figure 21. Theoretical determination of the dispersion of the second order coefficient d_{33} averaged per molecule (N) and poling field (E_p).

In a study by Kuzyk et al. (101), the extent of molecular ordering imposed by stress was determined by the sample's second harmonic emission. A dye doped polymer film was poled under mechanical stress. The ratio of two tensor components of the second order susceptibility, $a=\chi^{(2)}_{113}/\chi^{(2)}_{333}$, for this material varied with both the poling field and the magnitude of mechanical stress. In the absence of stress, the ratio was $a\approx0.3$, while for the film stressed by $\sim4\times10^7$ dyn/cm^2, the ratio was $a\approx0.7$. The values of an order parameter, calculated from this data were very different from empirical values obtained for the corresponding order parameter in liquid crystals and L-B films. This suggests that the nature of the molecular ordering created in the stressed film is different from that characteristic of these other two ordered systems.

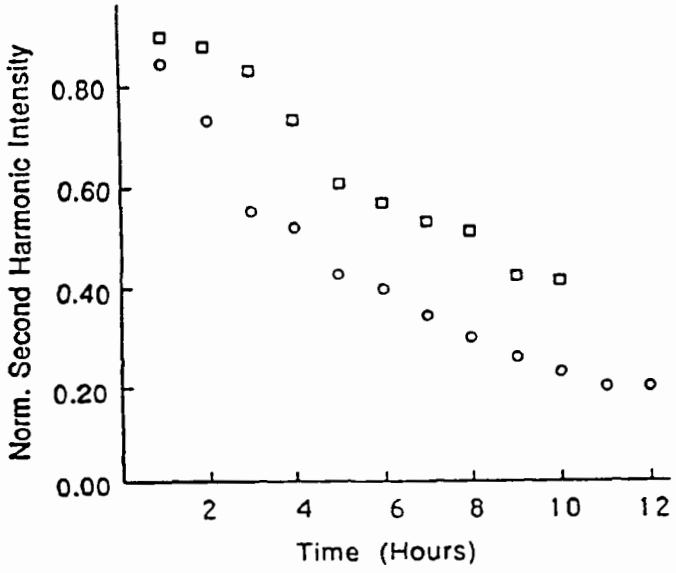

Figure 22. Decline in second harmonic signal with time following poling of PMMA (circles) and polystyrene (squares) films doped with 4% DANS. (Reproduced with permission from reference 102.)

The relaxation of the poled molecules in two different polymer host materials, both with the same guest, DANS, was compared by Hampsch et al. (102). The second harmonic intensity, emitted by spin-coated films of doped PMMA and polystyrene following poling, is displayed in Figure 22. Within a few hundred hours, films prepared from both hosts show nearly complete loss of the second harmonic signal, although the relaxation proceeds more rapidly in PMMA films. In an effort to prevent this relaxation of the active moieties to random orientations, some researchers have synthesized glassy polymers with sidechains possessing second order nonlinear properties. Ye et al. (103) have covalently attached nonlinear chromophores to a polystyrene

ckbone, obtaining values of the order of 3×10^{-9} esu for d_{33}. Several days later, the second harmonic signal emitted from such films kept at room temperature is reduced by a negligible amount, although at higher temperatures, the relaxation occurs more rapidly.

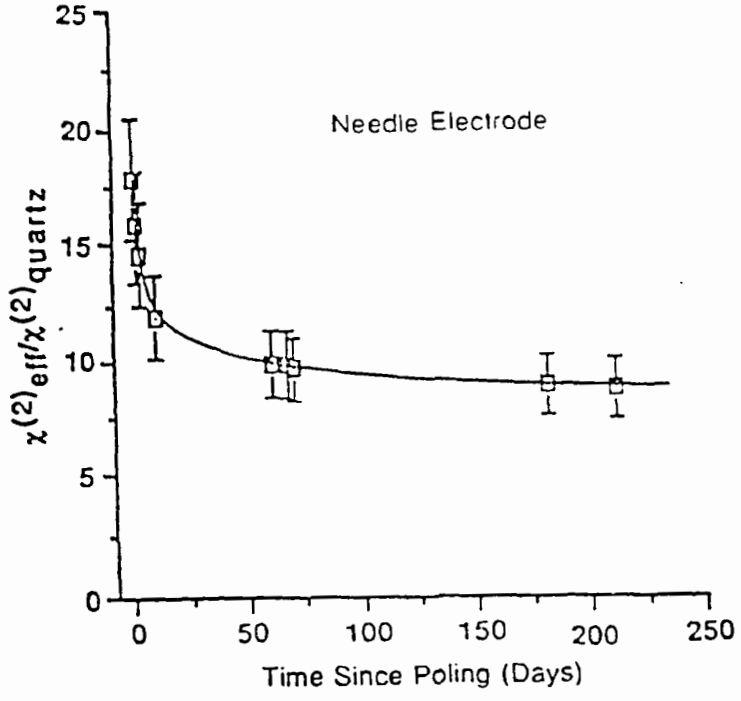

a.

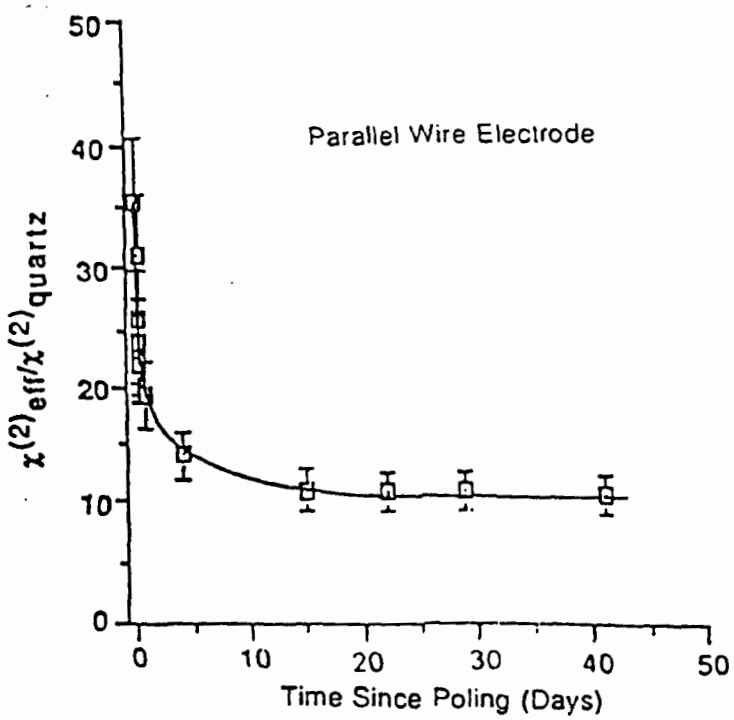

b.

Figure 23. The decay of the second order nonlinearity relative to quartz in PMMA films doped with Disperse Red 1 dye vs. time since poling. The sample in 23a was poled with a needle electrode, while the sample in 23b was poled by parallel wire electrodes.

Mortazavi et al. (104) conducted experiments to observe the effect on a guest-host film's second order properties when a corona discharge is used to pole the sample. Corona discharge occurs when an inhomogeneous electric field causes a partial breakdown in a gas between the electrodes. Two electrode configurations were tested: a needle electrode suspended perpendicular to the PMMA-Disperse Red1 film mounted on a grounded planar electrode, and a thin tungsten wire held parallel to the film-planar electrode assembly. The parallel wire electrode produced more controllable and consistent fields than the needle electrode. Films poled in the parallel wire electrode arrangement exhibited a higher optical quality while films were often permanently damaged by the first surge of current between the needle electrode and the film. During poling, samples were heated above the glass transition (about 110^{o} C) by a hot plate located below the planar electrode. Compressed air, fed through channels in the lower electrode, provided cooling to "freeze" the molecular orientation in the film once the sample was poled.

The effect of poling was visually evident and the films changed reversibly from a light orange to a red-violet transparency. Following removal of the field and cooling, the sample relaxed to its unpoled, orange form over a period of days. After a month, the sample nearly reverted to its unpoled state. The intensity of the second harmonic signal declined within days after poling (Figure 23), another indication of the material's relapse to a disordered state. Some residual orientation is indicated by the nearly constant level attained after several days as inferred from the second harmonic intensity. Despite these difficulties, the magnitudes of second harmonic coefficients measured in films poled by corona discharge are greater than those observed in films poled by conventional parallel plate electrodes.

Third Order Effects: Third Harmonics

Although second harmonics are restricted to noncentrosymmetric materials, third harmonics can arise in any medium. This complicates analysis of the output signal as not only the polymer sample of interest, but also the intervening air, water, and substrate materials contribute to the third harmonic. These background signals must be accounted for in order to obtain a useful characterization of the sample. For example, Berkovic et al. have calculated that the third order susceptibility of a LB monolayer must be at least comparable with that of a 280 Å depth of water (for 1.06 μ light incident at 60°) in order to be observable (32). This imposes a constraint on the materials in which third harmonics can be studied, using their experimental arrangement.

The same experimental setup used to investigate second harmonics from a sample can be modified for the generation of third harmonics. By transmitting the beam through a narrow bandpass filter just before and just after it passes the sample, third harmonics created in the optical elements can be restricted. However, as reported by Meredith et al. (105), third harmonic production in the air above the sample cannot be prevented. The detailed study by Kajzar and Messier (106) proposes an empirical air correction, dependent on focal length, laser frequency, angle, sample thickness, and the index of refraction of air and the material. Berkovic et al. (92) experimentally determined the ratio of the reflected third harmonic fields generated by water and air. This enabled them to sort the third harmonics due to a polydiacetylene LB monolayer from that of the background. Others minimize these environmental complications by placing the sample in a vacuum cell.

Table 3
Optical constants of polydiacetylenes and inorganic semiconductors. Values were obtained from reference 41.

Substance	Direction of light polarization	E_g (cm^{-1})	Refractive index (far from gap)	$\lvert\chi^{(3)}(\omega,\omega,\omega)\rvert$ (10^{-13} esu) at ω_1(2.62μm)	at ω_2(1.89 μm)	$\lvert\chi^{(3)}(\omega_1,\omega_1,\omega_1)\rvert/n^2$ (10^{-13} esu)
TCDU monomer	$\parallel \eta$	34250	1.58	• • •	1.2±0.6	0.48
	$\parallel \xi$	34700	1.53	• • •	1.1±0.6	0.47
TCDU polymer	$\parallel$ z (chains)	17900	1.80	370±140	700±500	110
	$\perp$z	• • •	1.65	<4	<7	• • •
PTS polymer	$\parallel$ z (chains)	15800	1.88	1600±1000	8500±5000	450
	$\perp$z	• • •	1.58	<20	<100	• • •
Germanium	(100)	5400	4.0	4000±2000 (at 10.6 μm)		250
GaAs	(100)	10900	3.2	480±290 (at 10.6μm)		50

An early experiment by Sauteret et al. (41) compared third harmonic generation in crystals of both monomer and polymer forms of the polydiacetylenes TCDU (Poly(5,7-dodecadiyne-1, 12-bis phenyl urethane)) and PTS with the aid of a quartz reference standard. Rotation of the polarization direction of the 1.89 μ source induced variations in the third harmonic signal emitted by the polymer crystals, while no (or minimal) variation was observed from monomer crystals. In monomer crystals, the components of $\chi^{(3)}$ along all directions are similar in magnitude. In the polymer crystals, the component along the polymer chain direction dominates the others by two orders of magnitude, and exceeds the monomer value by an even

ter factor, as documented in Table 3. The π-electrons along the polymer chains are sponsible for this pronounced, anisotropic increase in the value of $\chi^{(3)}$. On the basis of a one dimensional model of infinite polymer chains, theoretical values were derived by the authors that agreed qualitatively with the experimental results.

Kajzar et al. (107) reported the observation of third harmonics in L-B films of polydiacetylene oriented in the head-to-head Y-type symmetry coating one or both sides of quartz substrates. The path length of the 1.06 nm pulsed beam in the samples was varied by rotation with respect to the substrate normal as depicted in Figure 24. The third harmonic intensity emitted by the double-sided samples exhibited interference fringes. The harmonic waves from the substrate's opposite side were dephased by a variable amount, depending on sample rotation while traversing the quartz layer, due to dispersion. This effect was not observed in the single-sided samples. The resultant value of $\chi^{(3)}$ was about 2 orders of magnitude less than that obtained from single crystals by Sauteret et al. (41). In later studies Kajzar and Messier (108-110) conclude that this discrepancy may be attributed to the presence of a mixture of "blue" and "red" phases of polydiacetylene.

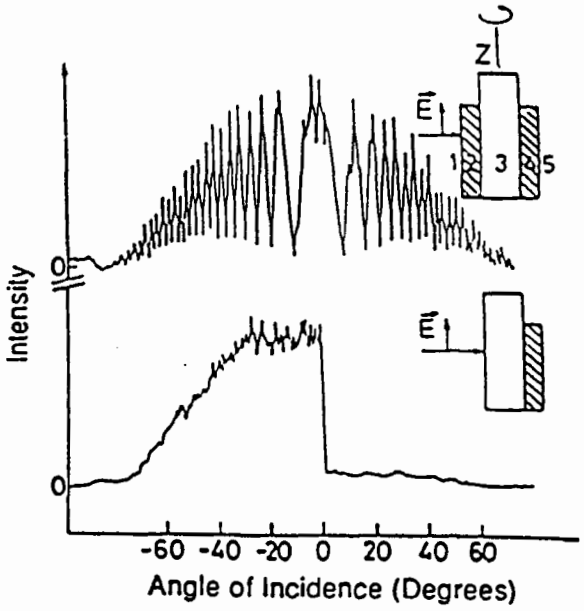

Figure 24. Dependence of third harmonic on incidence angle. Above: polymer on both faces of substrate. Below: polymer on one side only. (Reproduced with permission from reference 107.)

The dependence of the third order susceptibility of these polydiacetylene films on wavelength is presented in Figure 25 as determined by Kajzar et al. Two peaks appear prominently in the output: one at ~1.35 μ within the transparent region of the PDA spectrum; the other, represented by a single data point, at ~1.91 μ. These peaks correspond to two, and three

hoton resonances, respectively. In a separate study of third harmonic generation in polysilane films, in which measurements at two different incident frequencies were carried out, Kajzar et al. (111) attributed a high value of $\chi^{(3)}$ presumably due to a three photon resonance at one of the frequencies (~1.06 μ). At the other incident frequency (~1.91 μ), the $\chi^{(3)}$ value was below the threshold of detection. Kaino et al. (37, 38) have conducted studies on the spectroscopic behavior of the susceptibility $\chi^{(3)}$ based on third harmonic emission from thin films of poly-(2,5-dimethoxy *p*-phenylene vinylene) (MOPPV) and poly-(*p*-phenylene vinylene) (PPV). At wavelengths longer than about 2 μ, i.e. for frequencies much lower than the resonance frequencies, $\chi^{(3)}$ values for MOPPV and the blue form of polydiacetylene 3BCMU approach each other as shown in Figure 26.

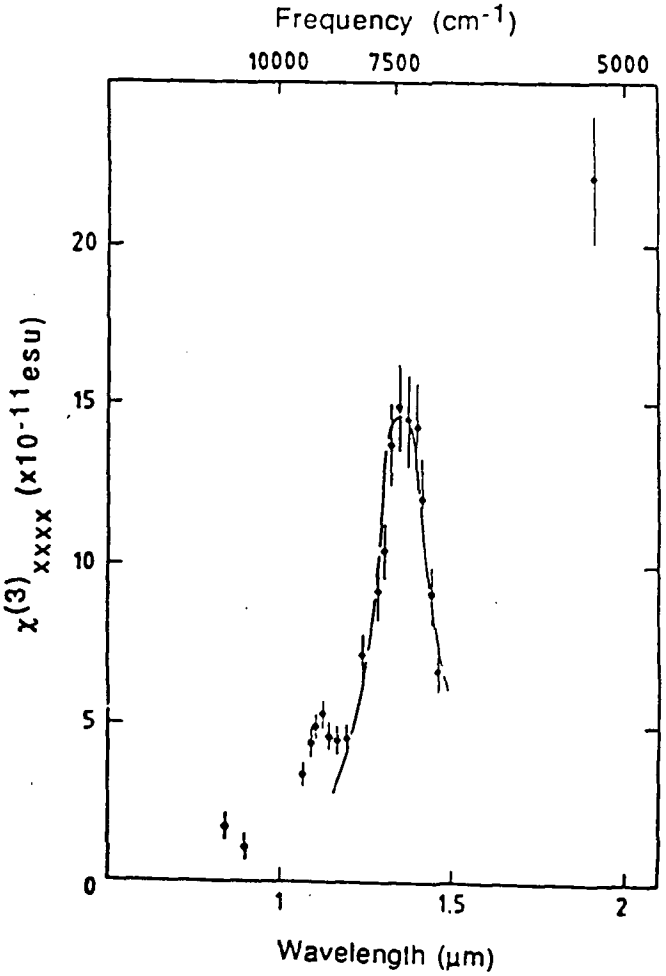

Figure 25. Cubic susceptibility $\chi^{(3)}_{xxxx}$ (-3ω;ω,ω,ω) of the blue form of polydiacetylene LB film, corrected for polymer disorder, as a function of incident laser wavelength. (Reproduced with permission from reference 109.)

Kajzar and Messier explored the relationship between optical nonlinearities and molecular chain length by analysis of the third harmonic signal emitted by a series of halogen substituted n-

anes (112). Figure 27 presents experimental and theoretical (solid lines) determinations of e susceptibility, $\chi^{(3)}$, as a function of increasing chain length in a variety of alkanes. At short chain lengths, the susceptibility is influenced by the character of the polar substituent, while as the chains are lengthened indefinitely, it approaches a common limiting value, $\chi^{(3)}_{\infty}$.

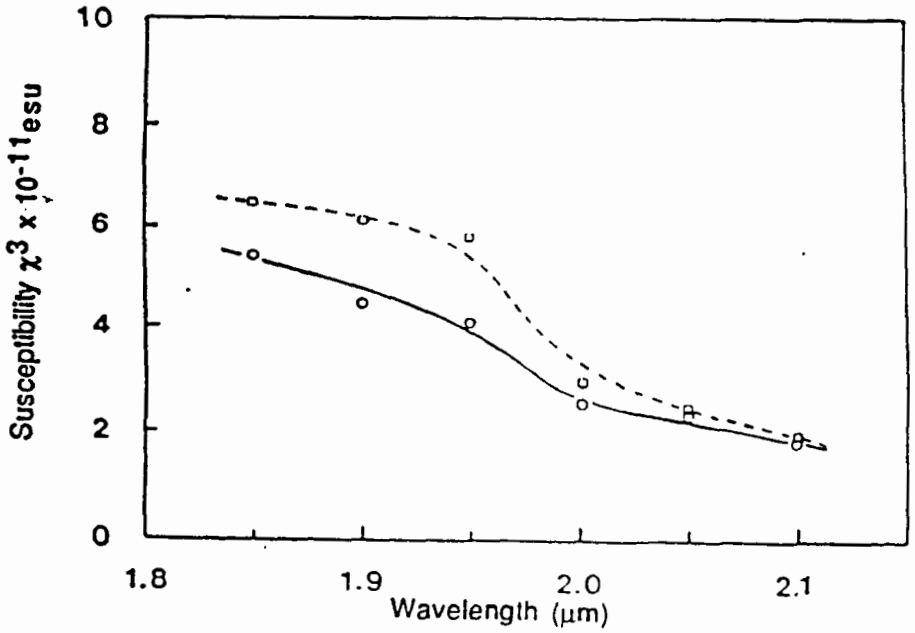

Figure 26. Variation of the third order susceptibility with the incident wavelength for MOPPV (circles) and poly(3 BCMU) polymer films. (Reproduced with permission from reference 38.)

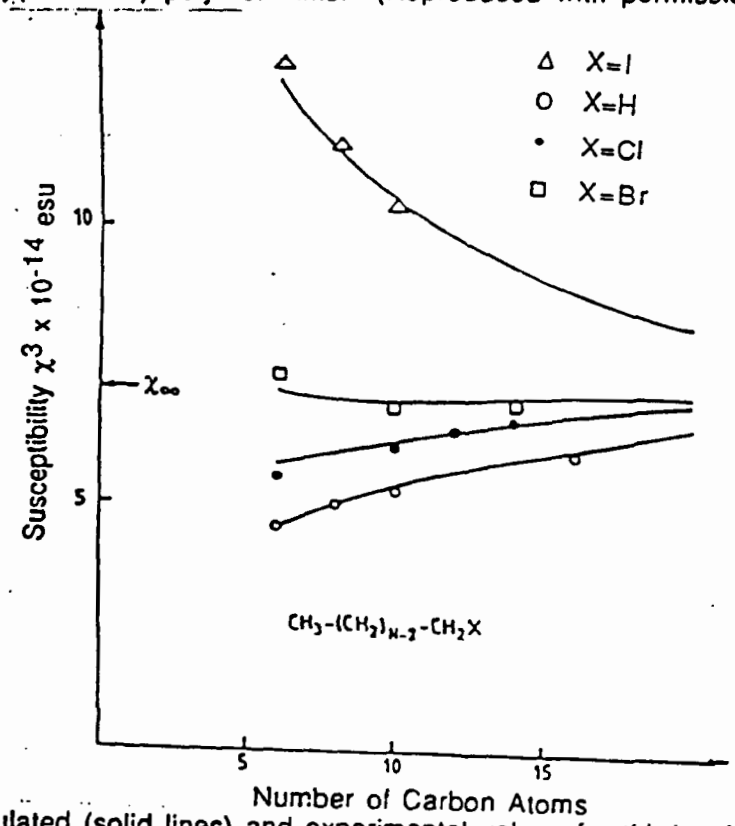

Figure 27. Calculated (solid lines) and experimental values for third order susceptibility as a function of carbon chain length in substituted alkanes. The limiting value, for infinite chain length, is χ_{∞}. (Reproduced with permission from reference 112.)

Gookin and Hicks (113) detected a third harmonic signal in the light which had scattered off the surface of a free standing *trans*-polyacetylene film held in vacuum. A third harmonic peak at 353 nm (the incident wavelength was 1.06 μ) was seen. Third harmonic generation has also been used by Sinclair et al. (39) to evaluate $\chi^{(3)}$ in polyacetylene films at 1.06 μ. In their experiment, the polyacetylene films were prepared on glass substrates. In another study of third harmonic emission from *trans*-polyacetylene films, Kajzar et al. (114) determined $\chi^{(3)}$ at different infrared wavelengths. Two sharp peaks in $\chi^{(3)}$, corresponding to two and three photon resonances, were observed (Figure 28).

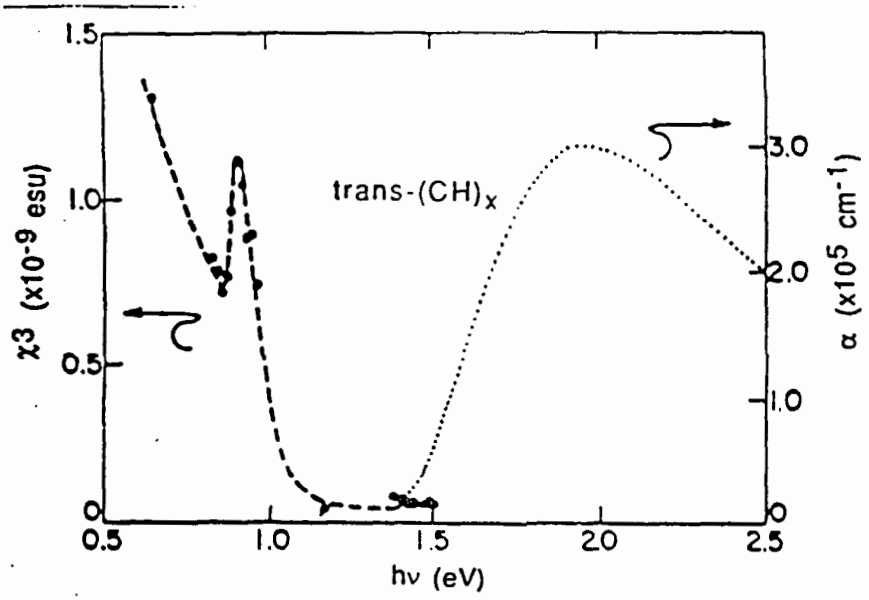

Figure 28. The closed circles are the absolute magnitude of the third order susceptibility parallel to the chains in trans-$(CH)_x$. The dashed line is to guide eye. The dotted line is the isotropic absorption coefficient. Reproduced with permission from reference 114.

A molecule's orientation and conformational changes can be deduced from the third harmonic signal it emits. Berkovic et al. (115, 92) were able to distinguish between monomer and polymerized films of diacetylenes floating on water by the intensity of the third harmonic. No signal was detected from the monomer film, due to its low nonlinear susceptibility. A significant enhancement in the nonlinear signal was seen upon polymerization. In a parallel experiment, an abrupt increase in the intensity of the third harmonic from a polydiacetylene film (4-BCMU) occurred when the film floating on the Langmuir trough was compressed. This corresponded to a phase change from the less conjugated yellow form of the film to a more conjugated red form, reflecting a direct connection between the magnitude of $\chi^{(3)}$ and

Baumert et al. (12) interpreted third harmonic emission from polysilane and polygermane films as indications of distinct, temperature-dependent, conformational changes. At low temperatures, the conjugated backbones of these polymers adopt a planar zigzag ordering which is stabilized by crystallization of the sidechains in place. At higher temperatures (42° C for poly(di-n-hexylsilane) and 12° C for poly(di-n-hexylgermane)), the sidechain crystalline organization melts, freeing the polymer backbones to adopt a more disordered conformation with a decreased conjugation length. While this conformational transition has been established through observation of the polymers' temperature-dependent absorption spectra, Baumert et al. demonstrated that the third harmonic, and hence, $\chi^{(3)}$, varies by a factor of six through this conformational change.

Third order nonlinear optical susceptibility $\chi^{(3)}$ has been evaluated using third harmonic generation for copolymers of azo dye substituted acrylic monomer and methylmethacrylate by Matsumoto et al. (116). The measured $\chi^{(3)}$ is 1.26×10^{-12} esu at 25.9 mol% azo dye monomer content in the copolymer. A linear relationship between $\chi^{(3)}$ and the dye-monomer content was observed.

Kerr Effect Measurements

The electric field applied to a sample induces changes in electronic arrangements which may be macroscopically evident as a change in the material's index of refraction. The magnitude of this change, which is proportional to the square of the applied field, can be used to determine the third order susceptibility, $\chi^{(3)}$, of a material.

Carter et al. (117) investigated the variation of refractive index with incident intensity in polydiacetylene L-B films deposited on silver-coated gratings etched on silicon wafers with depth of 500 Å and period of 5000 Å. The grating facilitates coupling of the laser beam into the polymer waveguide structure. Coupling occurs for a specific angle between the beam and the normal to the film surface. As the sample is rotated on a goniometer, the power of the reflected beam dips at the coupling angle. When the material's refractive index changes, the coupling angle will change as well. Figure 29 displays the shift in coupling angle incurred by a increase in incident pulse energy from 3×10^{-6} Joules to 1.3×10^{-5} Joules. A perturbation treatment expresses this change in coupling angle as $\Delta\theta_c = Cn_2(\Delta I)$, where C is a theoretically determined constant for the guide, n_2, the nonlinear index of refraction, and ΔI is the change in incident intensity. By this technique, the variation of nonlinear index n_2 with incident wavelengths ranging from near

the absorption edge (6700 Å) to 1.04 μ was measured. Figure 30 presents the resulting spectrum, and includes data from the two transverse electric modes, m=0 and m=1, excited in the waveguide. At the shorter wavelengths (<7000 Å) there appears to be a resonant enhancement in the refractive index change. In a similarly prepared PDA film the absorption edge was found at 7000 Å with a peak in the absorption at 6400 Å.

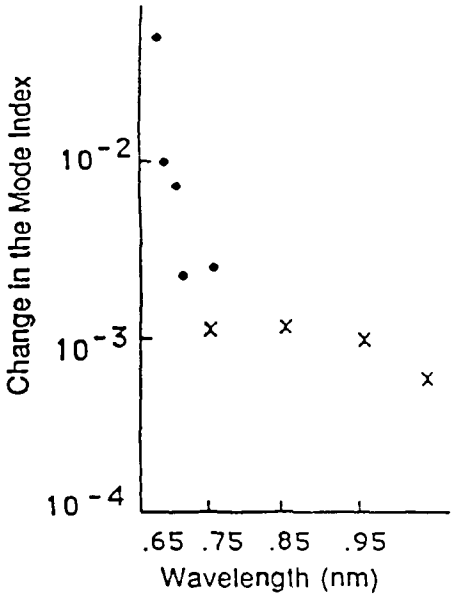

Figure 29. The change of refractive index with wavelength is plotted for polydiacetylene multilayer films (results from the m=1 mode are represented by dots; from the m=0 mode; by crosses). (Reproduced with permission from reference 117.)

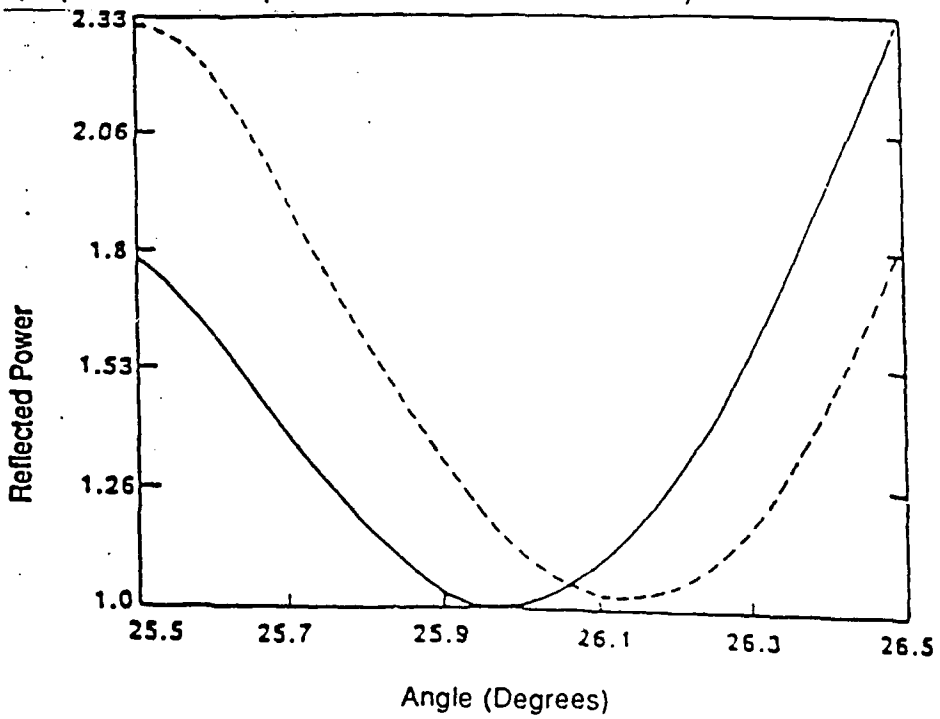

Figure 30. The change of refractive index with wavelength is plotted for polydiacetylene films (the variation of reflected power with angle is given for two input laser energies: 3×10^{-6} J/pulse (solid curve) and 1.3×10^{-5} J/pulse (dashed curve). (Reproduced with permission

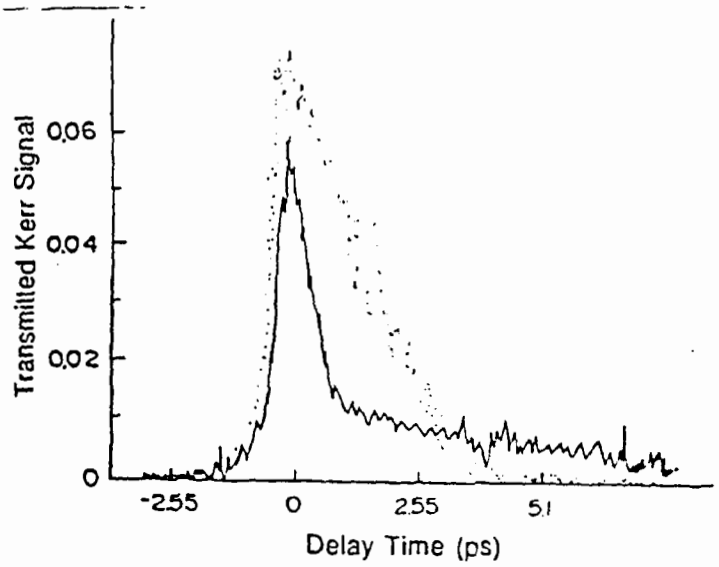

Figure 31. Kerr signal transmitted by 4 BCMU films (solid line) and a CS_2 Kerr gate (dashed) excited by 500 fs laser pulses. (Reproduced with permission from reference 118.)

Ho et al. (118 and 119) evaluated differences between fast and slow relaxation processes contributing to the optical Kerr effect in solutions of 4 BCMU-polydiacetylene in CH_2Cl_2. The samples were excited by a 625 nm pump beam, with a pulse width of 500 fs, and probed by a 760 nm pulse of the same duration. By selecting different wavelengths for pump and probe beams coherent effects were reduced and analysis of the data was simplified. Figure 31 shows the dependence of the ratio of the transmitted to probe intensities on the delay time between pump and probe pulses. The rise time of the transmission curve for the PDA solution is ~0.5 ps, while the decay time has a fast ~0.5 ps component and a slower ~6 ps component. The Kerr intensity is a function of $(\sin \delta\theta)^2$, where $\delta\theta$ is the phase shift. For small phase shifts this may be approximated as $\delta\theta^2 \propto (\delta n)^2 \propto e^{-2t/\tau}$ with δn as the change in the index of refraction and τ as the relaxation time. Thus the relaxation time of the Kerr medium is twice the decay time read directly from the graph, or about 12 ps. Photoluminescence studies (120, 121) identified a 10 ps relaxation time in PDA which closely corroborates the 12 ± 4 ps period of the slow Kerr process, indicating that photoexcited electrons may be responsible for this effect. The effect of resonant excitation on a polydiacetylene's third order nonlinearity was also demonstrated by the authors in a Kerr effect experiment. The pump beam was tuned to the polymer's absorption wavelength of 530 nm and the optical transmission was measured at 1060 nm. In Figure 32, the output curve from the film excited at resonance (solid line) is contrasted with the nonresonant

ersed situation (dashed line)--a pump beam of 1060 nm and a probe at 530 nm. The esonant relaxation time was 12 ps, corresponding again to the characteristic time of photoexcited electronic processes. In these polydiacetylene samples, the value of the nonlinear index n_2 varied linearly with absorption coefficient, yielding a nonresonant value for $\chi^{(3)}$ of 3×10^{-10}esu.

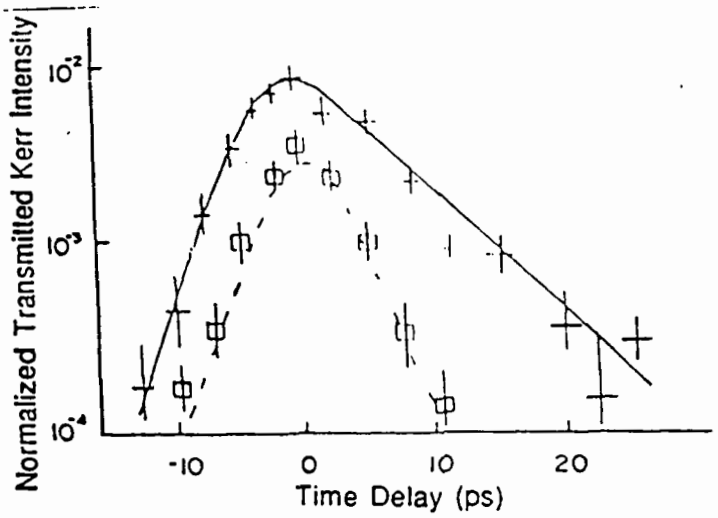

Figure 32. Resonant and nonresonant Kerr transmitted signal of 0.1% 4 BCMU in CH_2Cl_2. The squares show the data for nonresonant (1.06 μ) excitation and crosses show the data for resonant excitation (0.53 μ).

Uchiki and Kobayashi (122) have employed a straightforward technique for experimentally determining real and imaginary parts of $\chi^{(3)}$. A Fabry-Perot cavity is created by sandwiching a thin film of the candidate material between partially transparent aluminum films, all deposited on a glass substrate. The aluminum films served both as electrodes and mirrors for the cavity. A square wave amplitude of 10V applied across the aluminum films induced changes in transmittance, which were recorded by a detector and a lock-in amplifier. The change in transmittance with wavelength for a cavity filled with a guest-host film of polycarbonate doped with DEANS is displayed in Figure 33. At wavelengths away from this material's absorption edge (600 nm), change in transmittance is still appreciable.

The normalized change in transmittance may be expanded as

$$\delta T/T = [(\partial T/\partial n)/T]\delta n + [(\partial T/\partial k)/T]\delta k$$

where n and k are the real and imaginary parts of the refractive index and δn and δk are the field-induced changes in n and k. Through theoretical determinations of the terms in brackets,

alues for Δn and Δk, which can be converted to the real and imaginary parts of $\chi^{(3)}$, were culated. Figure 34 presents the results of these calculations. In the absence of an applied eld, absorbance drops essentially to zero at wavelengths longer than 600 nm. However, for an applied field of 70 kV/cm, there is still a contribution from the imaginary part, Δk, at wavelengths larger than 600 nm. Uchiki et al. obtained a value of $(6.3+4.0i)\times10^{-12}$ esu for $\chi^{(3)}$ from this data.

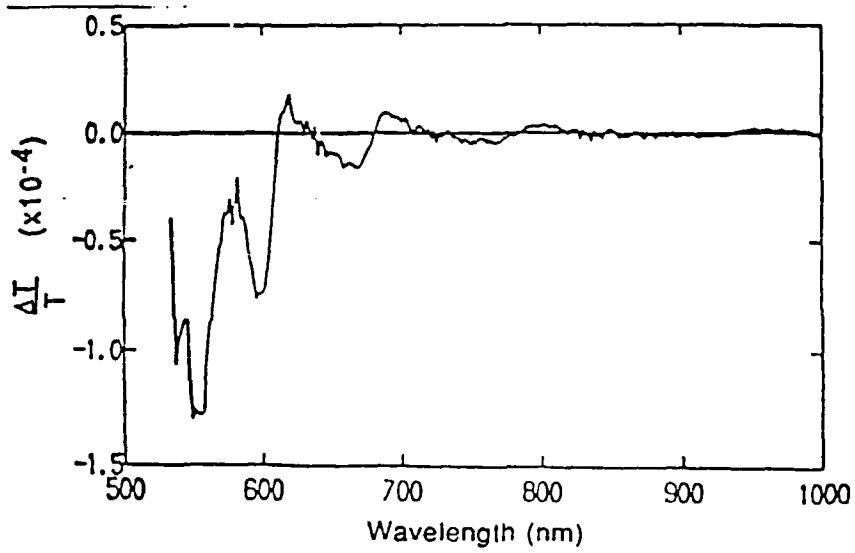

Figure 33. The normalized variation in transmittance with wavelength for a DEANS guest-host material subjected to a 500 Hz square wave potential (10 V peak to peak). (Reproduced with permission of reference 122.)

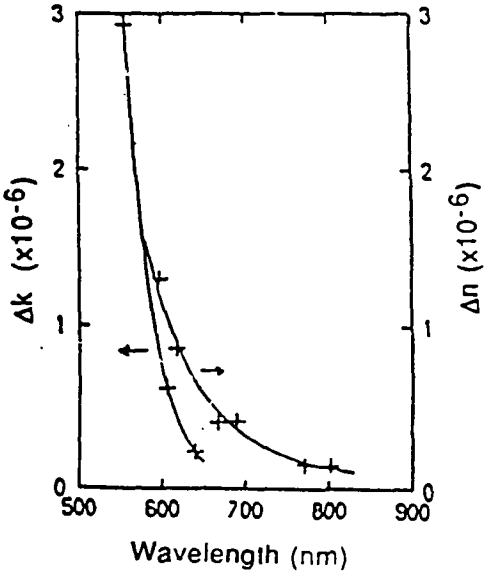

Figure 34. Changes in the imaginary (Δk; left curve) and real (Δn; right curve) parts of the refractive index is plotted against wavelength. (Reproduced with permission from reference 122.)

Kuzyk and Dirk (123) have adapted interferometric techniques to evaluate the nonlinear optical properties of guest-host polymer films. A film formed from a PMMA matrix doped with cyano vinyl azo dye is inserted in one arm of a Mach-Zehnder interferometer while rotation of a glass slide positioned in the other arm varies the relative phase between the arms. An oscillating electric field, applied to the film in the direction of the beam, modulates the phase in the sample arm. By recording the transmitted intensity of both the laser beam and the modulation, the second and third order susceptibilities may be determined. The value of $\chi^{(3)}$ obtained for this sample is 1.26×10^{-12} esu. Singer et al. (124) employed a similar method for the study of corona-poled polymer films to evaluate the linear electro-optic coefficient.

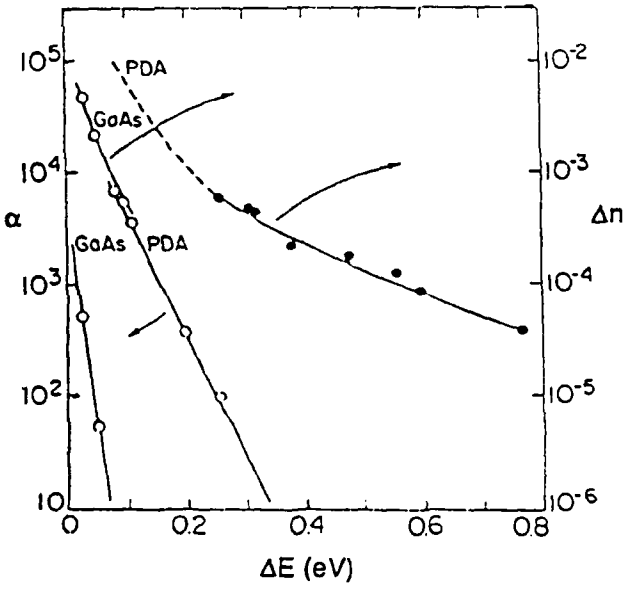

Figure 35. Plots of refractive index change (Δn) vs detuning below the exciton peak. Measured values PDA-PTS (solid circles) and literature values for GaAs MQW (open circles) are scaled to an applied field of 10^5V/cm. Also plotted are literature values of the absorption coefficients (α) for GaAs and PDA-PTS. (Reproduced with permission from reference 125.)

Recently Green et al. (125) have performed Kerr effect experiments on a single crystal of PTS at wavelengths slightly longer than the exciton absorption peak. By applying an 800 Hz unipolar sine wave voltage across the film via deposited gold electrodes, fields of 4×10^3 to 4×10^4 V/cm were created. The sample, was placed between crossed polarizers, and illuminated with light from a monochromator. The modulation in the light beam was measured at twice the frequency of the modulating field using a detector and a lock in amplifier. From the change in transmittance, which depended quadratically on the field (as expected in the Kerr effect), the

-induced change in refractive index, Δn, was calculated. The values for Δn, plotted in Figure against detuning, or energy below the exciton peak, correlate with previous determinations based on electroreflectance experiments.

Raman Scattering

Raman scattering has been employed in the investigation of polymer chain dynamics and conformation. Resonance, surface enhanced as well as stimulated Raman scattering effects can be used to enhance the low signal levels typically plaguing Raman processes. Raman scattering has been demonstrated from bilayers and multilayers of polymeric L-B films using surface enhanced Raman scattering. Experiments in bulk materials and solutions have yielded information about third order nonlinearity in certain polymers.

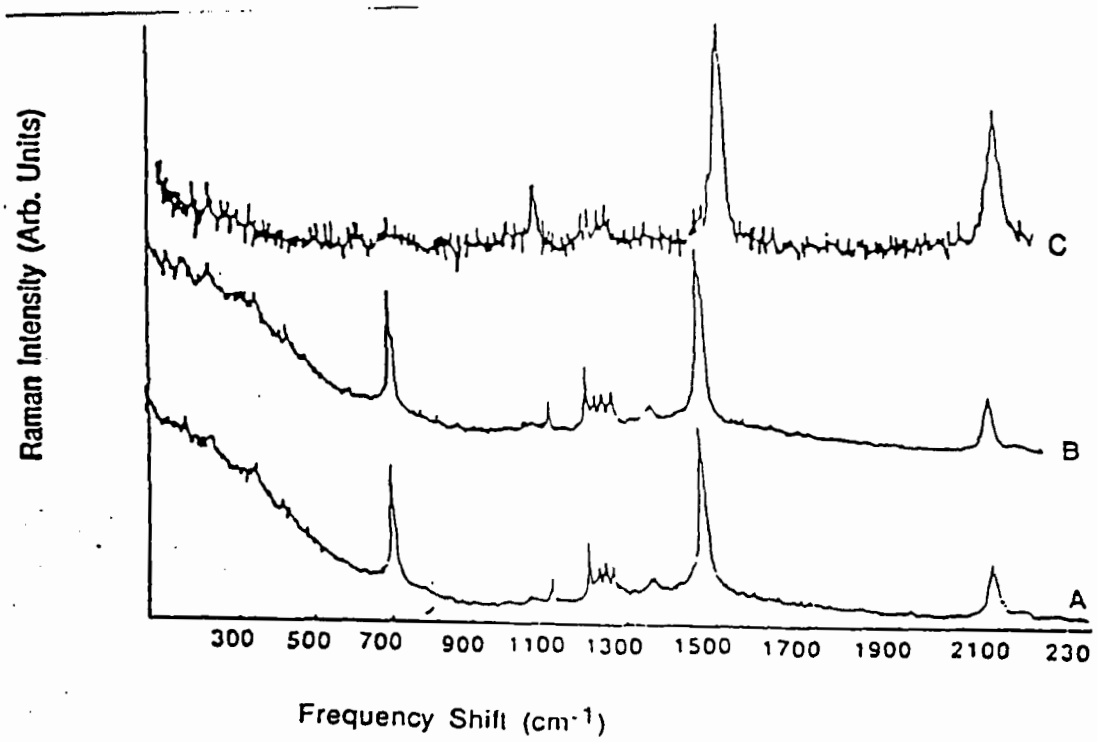

Figure 36. Raman spectra from one-, two- and three- bilayer films measured by surface-enhanced Raman scattering. The incident wavelength was 6328 Å. (Reproduced with permission from reference 127.)

Surface-enhanced Raman scattering from 15-8 polydiacetylene films stimulated by a 6238 Å laser was demonstrated by Chen et al. (126). These films were prepared by complete polymerization at the air-water interface into the red phase and subsequently transferred to a glass slide coated with a discontinuous thin film of silver. While the Raman spectra, displayed in

36, of multiple (two- and three-) bilayers are similar, that of the single bilayer film is inct. The two major Raman peaks, corresponding to C=C and C≡C stretch modes of the ackbone, are shifted in position from 1521 cm^{-1} to 1456 cm^{-1}, and from 2123 cm^{-1} to 2078 cm^{-1}, respectively. This downshift in frequency may be accounted for by the delocalization of polymer backbone electrons which was facilitated in the multilayer assemblies. It was concluded that the first bilayer covering the silver coated surface is significantly more disordered. The backbone retains the electronic structure of the red phase polydiacetylene. As multilayers are organized a more ordered blue phase component increases. Burzynski et al. (128) have also observed Raman scattering from L-B polydiacetylene films in more ordered blue films of polydiacetylene. The waveguide geometry, employed in their experiment provides a larger interaction length and hence increased sensitivity.

Excitation of a sample by a coherent source, through CSRS or CARS mechanisms, induces vibrational behavior detectable in the output spectrum. In addition to yielding Raman frequency shifts, these processes may reveal the third order susceptibility and hyperpolarizability of the sample material. Two laser beams incident on the sample with frequencies ω_1 and ω_2 give rise to a third, ω_3, by the mechanism of three wave mixing. Chance et al. (129, 130) investigated the Raman spectra from polydiacetylene solutions of 3 and 4-BCMU in poor and good solvents. BCMU undergoes a solvatochromic transition going from good to poor solvents. A blue solution is obtained for 3 BCMU in a chloroform-hexane solvent. A yellow solution is realized in pure chloroform for 4-BCMU and a red solution when 4-BCMU is dissolved in chloroform hexane mixture. The output frequency corresponding to $2\omega_1-\omega_2=\omega_3$ was monitored in both the Stokes (CSRS; $\omega_2>\omega_1>\omega_3$) and anti-Stokes (CARS; $\omega_3>\omega_1>\omega_2$) modes. The ratio of the ω_3 output intensities for the yellow polymer solution, normalized by the intensity emitted by the pure solvent, are recorded in Figure 37 as a function of increasing polymer concentration, for two values of ω_1. By fitting these curves with theory, the real and imaginary parts of the two photon hyperpolarizability γ_T were evaluated, as shown in Figure 38. The close fit between theoretical curves (solid lines) and the experimental data points was used to emphasize the validity of a two-photon absorption model in describing the behavior of polydiacetylenes in solution.

Hetherington et al. (131) demonstrated CARS emission from optical waveguides of a 2 μ thin polystyrene film. Prisms coupled beams from two lasers of different frequencies into the film. By varying the angles between the beams the CSRS phase matching angle (~1^o) could be

rmined. The prominent peak of the CSRS spectrum shown in Figure 39 occurs at 1000 cm^{-1}, hich corresponds to the ring vibration of polystyrene. A relatively high efficiency of ~$2x10^{-3}$ was obtained for conversion into the Raman shifted frequency.

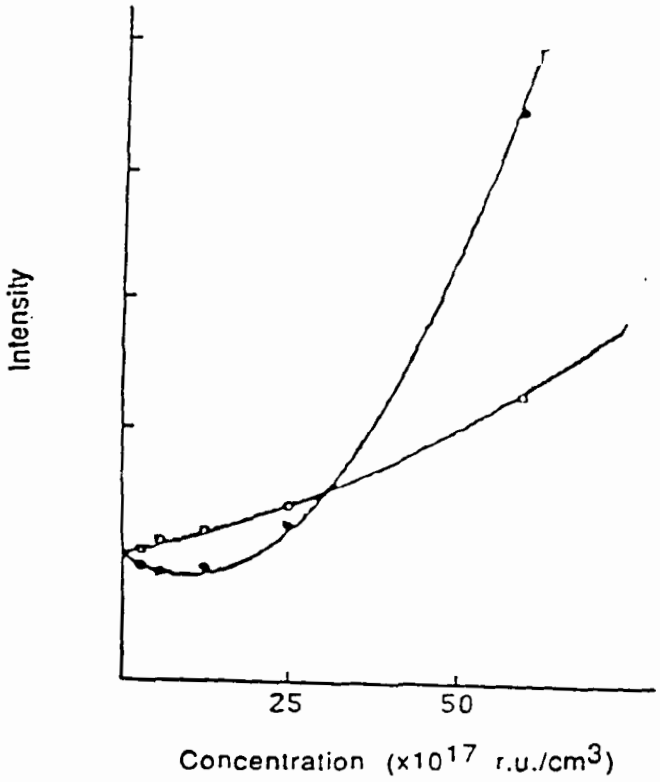

Figure 37. Variation in output intensity with polymer concentration for a 4 BCMU-PDA solution at two values of incident wavelength (closed dots at 32362 cm^{-1}; open dots at 26554 cm^{-1}). Solid lines are theoretical fits. (Reproduced with permission from reference 129.)

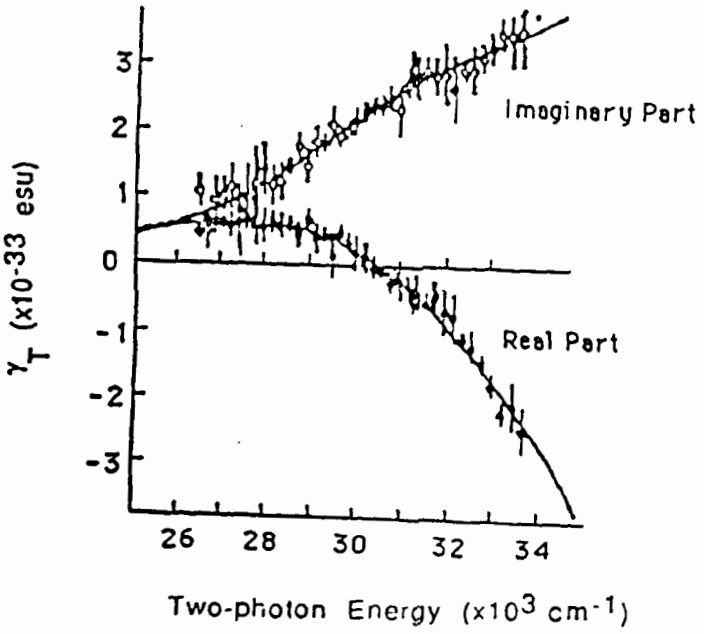

Figure 38. Change in the real (solid dots) and imaginary (open dots) parts of the two-photon hyperpolarizability, γ_T, with the two-photon energy in a PDA solution. The solid lines are theoretical fits. (Reproduced with permission from reference 130.)

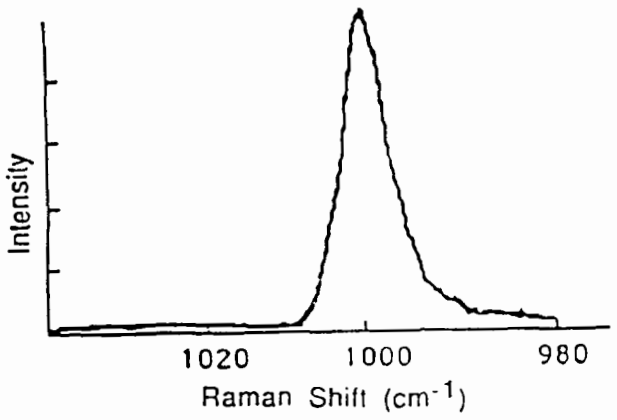

Figure 39. The CSRS spectra of a polystyrene waveguide.

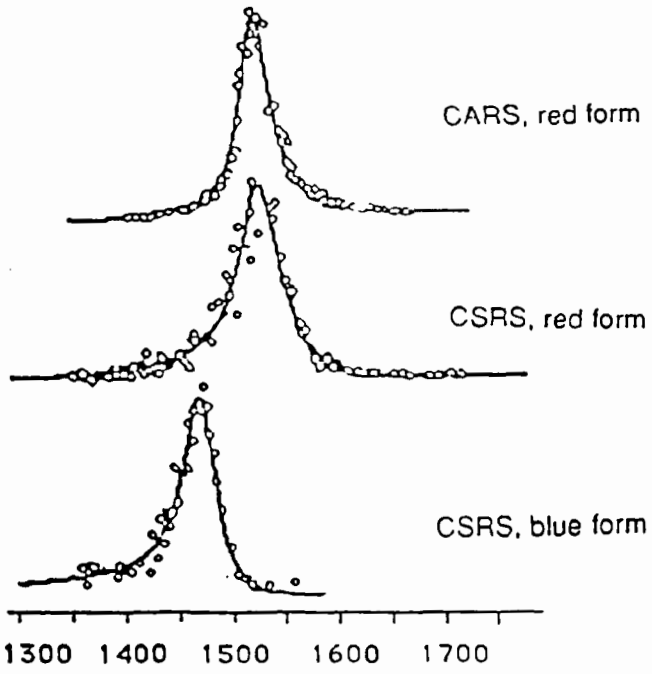

Figure 40. CSRS peak from the blue form of 4 BCMU at 1472 cm^{-1} and CSRS and CARS peaks from the red form of 4 BCMU at 1530 cm^{-1}. (Reproduced with permission from reference 132.)

The vibrational resonances of the polydiacetylene 4-BCMU in a blue, ordered and a red amorphous form by CSRS and CARS were investigated by Swiatkiewicz et al. (132) by time resolved techniques (133). Film samples subjected to two incident frequencies, ω_1 and $\omega_2(\omega_2>\omega_1)$, from synchronously pumped picosecond dye lasers produced signals at $\omega_4=2\omega_2-\omega_1$ for CSRS or at $\omega_3=2\omega_1-\omega_2$ for CARS. The authors focussed their study on the Raman emission corresponding to the C=C stretching of the polymer backbone. This peak occurred at 1472 cm^{-1}

CSRS in the blue form and at 1530 cm^{-1} for CSRS and CARS in the red form, as represented in Figure 40. In theoretical fits to the lineshapes of Figure 40, the authors concluded that the nonresonant component of the third order susceptibility, $\chi^{(3)}_{nr}$ greatly exceeded the two photon absorption component, $\chi^{(3)}_{tr}$. This result for two photon resonance in thin solid films differs from the behavior observed for polydiacetylene solutions (129).

Degenerate Four-Wave-Mixing and Pump-Probe Experiments

The third order susceptibility and time response behavior of many nonlinear materials have been characterized through degenerate four-wave mixing experiments with both continuous wave and pulsed laser sources. The production of a signal through degenerate four-wave mixing in the transparent regime of polymeric systems, however, requires high intensities, which are only available from pulsed lasers. Most investigations have been conducted with pulses of nanosecond or shorter duration, thus minimizing thermal effects and providing information about the medium's relaxation mechanisms. If the relaxation time of a medium is of the order of hundreds of femtoseconds, a nonresonant electronic third order process is probably responsible. Longer relaxation times, on the order of picoseconds or longer, are associated with vibrational relaxations of resonant excitations or orientational processes.

In pump-probe experiments, a sample is excited by a pump beam, and probed by a beam of much weaker intensity for changes in transmission or reflection. The frequency of both the pump and probe beams can be tuned independently, facilitating the production of time-resolved spectra by either transmission or reflection. Typically, these experiments are used to probe changes in a material's absorption and index of refraction near a resonant excitation as a function of intensity. These techniques may also be used to monitor Stark shifts in a material.

A subpicosecond response time for π–electron conjugated systems was confirmed through degenerate four-wave-mixing by Rao et al. (134) in poly-*p*-phenylene benzo-bis-thiazole (PBT) films. Photon energies less than that corresponding to the absorption edge (~560 nm) yielded subpicosecond response time for the polymer's third order nonlinear susceptibility. No evidence for a slow decay component was established, even when the probe or backward pump beams were horizontally polarized, indicating the involvement of electronic $\chi^{(3)}$ processes. Two components of the third order susceptibility, derived with CS_2 as a standard, were $\chi^{(3)}_{1111} = 5.4 \times 10^{-12}$ esu and $\chi^{(3)}_{2222} = 7.2 \times 10^{-12}$ esu.

Carter et al. (55, 127, 135, 136) have observed the relaxation time and other third order properties of micron-thin polydiacetylene crystals through phase-matched four-wave-mixing. The four wave mixing experiment was carried out with incident pulse widths of either 6 ps (open circles) or 300 fs (dots) at a wavelength of 6500 Å. The normalized power of the diffracted beam is plotted against T_d, the delay time of one of the incident pulses, in Figure 41. Pulses arriving with a positive time delay--after the grating's formation--diffract off the residual grating. The peak's asymmetry in time is due to this effect. The data indicates an off resonance relaxation time shorter than the duration of the pulse (300 fs) and an excited life time of 1.8 ps.

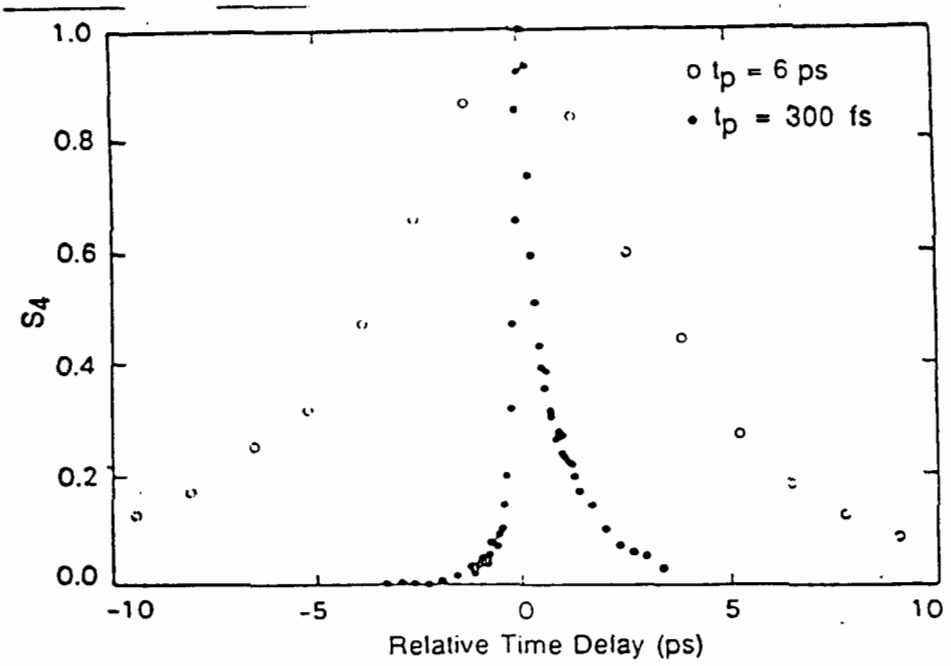

Figure 41. The four-wave mixing signal S_4 as a function of time delay of one of the incident laser beams. The open circles represent results for incident laser pulses 6 psec in duration, and the filled circles represent results for 300-fsec pulses. For both sets of data the laser wavelength was 6500 Å in resonance with the excitonic state in PDA. (Reproduced with permission from reference 135.)

In another experiment employing 60 fs pulses, Carter et al. observed a shorter 100 fs relaxation time in addition to the longer 1.8 ps relaxation time. Upon excitation the molecules may be raised to an energy level which decays in 100 fs through vibrational coupling to a state with relaxation time of 1.8 ps. Additional experiments at different wavelengths in the nonresonant regime (55, 135, 136) established the ultrafast temporal response of polydiacetylenes, although definitive values for the relaxation times remained undetermined. Dennis et al. (137) and Rao et al. (138) also attempted to resolve the relaxation time, but were limited by the laser pulse width.

In the experiments described above, the laser pulses, short as they are, are still unable to probe the relaxation time of polydiacetylene in its transparent regime. By exciting polydiacetylene films with beams from an incoherent laser interacting in a degenerate four-wave-mixing geometry, Hattori and Kobayashi (139) have resolved values for relaxation times at two wavelengths (648 and 582 nm). The pump beams from such a broad band laser has a coherence length of only a few microns corresponding to a coherence time of only tens of femtosecond. A variable time delay was introduced between the two pump beams which interfered to create a transient grating. Photodiodes detected the diffracted output intensity along two directions: $2n_1$-n_2 and $2n_2$-n_1, where n_1 and n_2 are the wave vectors of the pump beams. When the polarizations of the two exciting beams are perpendicular, the contribution to the output signal from the thermal grating itself is eliminated, thus output is entirely due to electronic nonlinear susceptibilities. By plotting diffracted intensity against the time delay, as in Figure 42, response times of less than 100 fs was resolved.

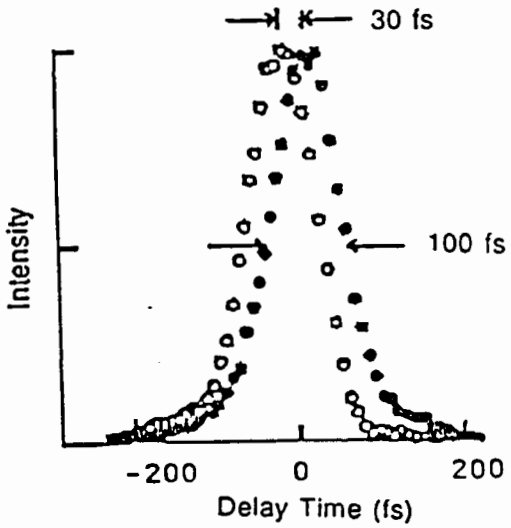

Figure 42. Time delay curve of the degenerate four-wave-mixing signal emitted by PDA films. Open circles represent the intensity of the signal diffracted in the direction $2n_1$-n_2; for closed circles, along direction $2n_2$-n_1. The exciting wavelength is 648 nm. (Reproduced with permission from reference 139.)

Employing degenerate four-wave-mixing, Wang and Mahler (140) inferred a three level mechanism explaining the nonlinear behavior of a sample containing 50 Å CdS particles embedded in a polymer film by comparing pump and signal power. Both the absorption of the laser pump beams and the degenerate four-wave mixing signal saturated at the same power level (a few

MW/cm^2). Measurements recorded by Maloney (141) in polymer solutions, by Rao et al. (134) in thin films of poly-*p*-phenylene benzo-bis-thiazole and by Fujiwara and Nakagawa (142) in a guest-host sample of methyl red-doped PMMA and gelatin, have revealed evidence pertaining to the excited states, as well as a measure of nonlinear susceptibility and its molecular counterpart γ.

Yang et al. (143) using four wave mixing have obtained relaxation times of less than 12 ps for polycondensed thiophene based polymers. In addition, they measured the dispersion of $\chi^{(3)}$ in these media by exciting the sample with a range of input frequencies. In parallel studies of polysilanes, Yang et al. (144) and McGraw and Siegman (145) have measured electronic contributions to $\chi^{(3)}$ and placed upper bounds on the medium's relaxation time.

Degenerate four-wave-mixing has been employed by Zhao et al. (146) to examine the effect of increasing the number of repeat units, N, in the polymer chain on the $\chi^{(3)}$ of oligomers of thiophene. Solutions of thiophene oligomers of various lengths, in benzene were investigated using a Nd: YAG laser in the medium's transparent regime. The solution's nonlinear susceptibility $\chi^{(3)}$, increased rapidly as the number of repeat units in the oligomers increased as shown in Figure 43. Their data suggests that high values of $\chi^{(3)}$, on the order of 10^{-9} esu, may be attainable, not only from long polymer chains but also from relatively short oligomers, of about ten repeat units.

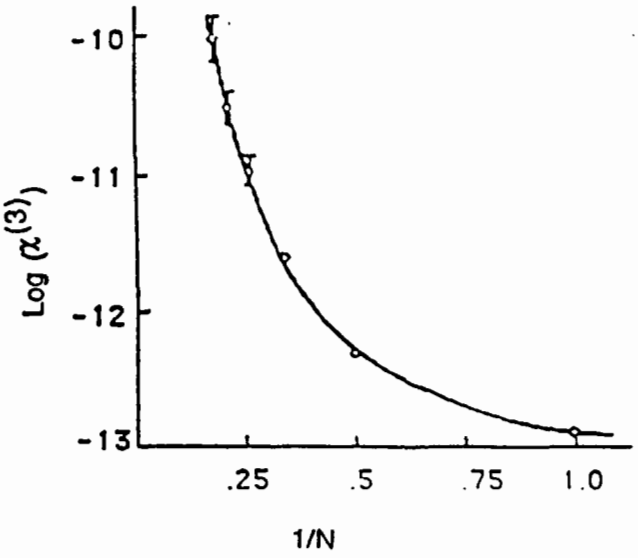

Figure 43. Variation in the log of $\chi^{(3)}$ with 1/N, where N is the number of thiophene repeat units. (Reproduced with permission from 146.)

Cong et al. (147) have also employed degenerate four-wave mixing to establish relationships between nonlinear response and molecular structure. A 532 nm pulsed beam was used to study a polydiacetylene solution (poly-4-BCMU) while it underwent a thermally induced transition from a red solution (absorption at 540 nm) to a yellow solution (absorption at 460 nm). This transition of poly-4-BCMU is accompanied by the breaking of hydrogen bonds and a reduction in conjugation length in the molecule (148, 149). The disparity in diffracted wave intensities between the more conjugated red form as compared to the yellow form confirms other evidence associating extensive conjugation with pronounced optical nonlinearity. Degenerate four-wave-mixing thus provided a sensitive, direct probe of this transition.

In other studies, Kobayashi et al. have employed the pump-probe technique to determine the lifetime of an excited singlet transition in guest-host films of DEANS (150). They have also studied the temporal features of the reflection spectra of polydiacetylene crystals (151, 152). Upon excitation by two different pump frequencies (266 and 532 nm), a probe reflected from the crystals revealed nearly identical exponential decay curves with time constants, τ, of about a microsecond. The fact that the curves are similar implies that a broad band of frequencies can elicit the same dynamical response from the system. In another experiment, by subjecting polydiacetylene single crystals to nanosecond length pump pulses, Kobayashi et al. (153) have observed decay of the photoexcited state with a time constant of ~0.75 μs.

Greene et al. (154) developed a technique for measuring a polymer sample's change in reflectivity following excitation by a pump pulse which substantially improves the experimental signal-to-noise ratio. As in the degenerate four-wave-mixing experiments described above, two spatially and temporally coincident 1.97 eV pulses overlap at the sample, creating a temporary intensity grating. A third, time delayed probe pulse, derived from a filtered white light continuum pulse also centered at 1.97 eV, diffracts off the grating and is detected. The input energy of 1.97 eV, coincides with a sharp resonant peak in the reflection and absorption spectra of their polydiacetylene sample. This exciton resonance peak exhibits such a pronounced absorption that effective transmission experiments would require thinner (100 Å) crystals than were available and thus, the samples were examined by reflection.

Figure 44 displays the normalized diffraction efficiency as a function of time delay. The polymer molecules relax to their ground state in a time of 2 ps, in close agreement with the results obtained by Carter et al. (135). The authors associate this 2 ps recovery time with the

lifetime of excitons created in the polymer chain by the 2 eV pump stimulus. From the reflectivity change and by applying the theory of Schmitt Rink et al. (155) developed to discuss the behavior of exciton in inorganic semiconductors, they deduce the exciton dimension in this PDA to be 33 Å. The nonlinear index of refraction was found to be 10^{-8} cm^2/watt. In another study (156), they obtained singlet excitation lifetimes of 0.8 ± 0.2 ps for PDA crystals at 300 K and 1.1 ± 0.2 ps at 5 K. The authors suggest that this non-radiative relaxation proceeds through a conformationally relaxed singlet state, persisting for about 1.0 and 3.4 ps at 300 K and 5 K, respectively. No evidence of triplet exciton formation via the singlet exciton was apparent, although rapid triplet exciton formation followed 3.94 eV excitation.

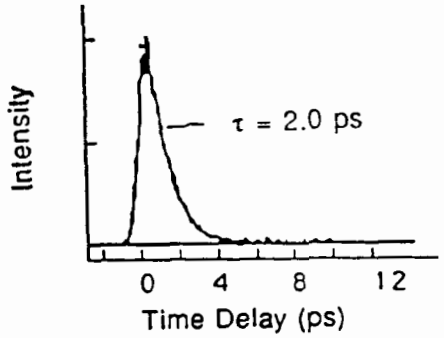

Figure 44. Dependence of the diffracted beam intensity on the time delay between pump and probe beams. A ground state recovery time of 2.0 ps is evident in the decay part of the curve. (Reproduced with permission from reference 154.)

In another experiment Green et al. (157) have investigated phonon mediated optical nonlinearity in PTS. Pump-probe experiments were performed on very thin samples of PTS-PDA. The differential optical density ΔOD was monitored through the region of exciton absorption as the pump beam was tuned through resonance. Figure 45 show the optical density of a 200 Å thick PTS single crystal with the beam polarized in the polymer chain direction. The middle and lower traces show the differential optical density for the nonresonant and the resonant excitation respectively. The differential optical density spectra for resonance and off resonance excitations are quite different from each other and different completely from those obtained from analogous experiments on GaAs-AlGaAs multiquantum wells as observed by Mysyrowicz, et al. (158). Figure 46 shows the bleaching of exciton absorption vs pump detuning for PTS. The two maxima correspond to phonon energies obtained by Raman scattering. Thus according to the authors whereas in multiquantum well structures the near resonant nonlinearity results from interaction

between virtual excitons, in PTS-PDA it apparently results from interactions in which optical phonons are involved. Kobayashi et al. (159) and Heritage et al. (160) have also investigated phonon-mediated effects in PDAs.

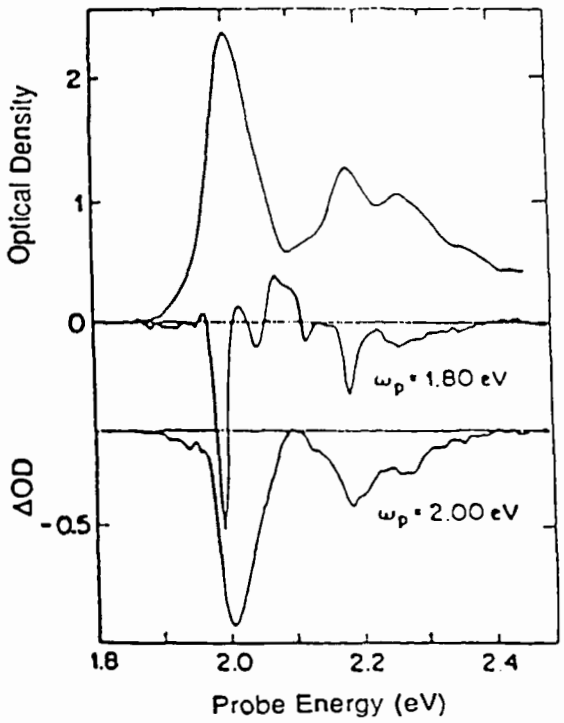

Figure 45. The dependence of optical density in 200 Å polydiacetylene films on the energy of the probe beam. The differential OD is given when a pump beam of energy below resonance (1.8 eV; middle) or at resonance (2.0 eV; bottom) excite the film. (Reproduced with permission from reference 157.)

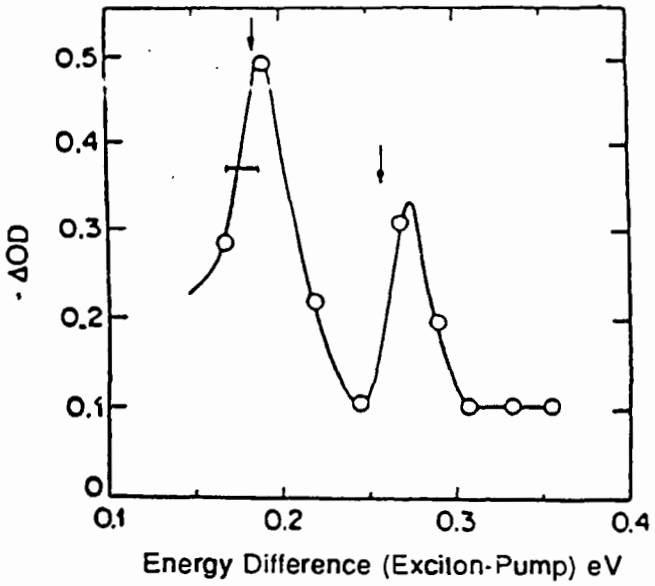

Figure 46. The determining of the pump beam energy from resonance is plotted against the differential optical density for the thin polydiacetylene film. The arrows mark the energies of phonons obtained from Raman spectra.

Saturation of absorption and third order nonlinear effects have been investigated in Langmuir-Blodgett films of polydiacetylene by Kajzar et al. (161). Picosecond time resolved measurements at 583 nm were performed. Using photoacoustic spectroscopy technique the authors have obtained the imaginary part of the third order susceptibility $\chi^{(3)}$. The photoacoustic method enables them directly to compute $(\delta\alpha/\alpha)$ where $\delta\alpha$ is the change in absorption and α the linear absorption co-efficient. Figure 47 shows the bleaching signal from polydiacetylene as a function of the pump-probe delay. The magnitude of $\chi^{(3)}$ was found to be greater than 10^{-8} esu and the recovery time is less than 3 psec.

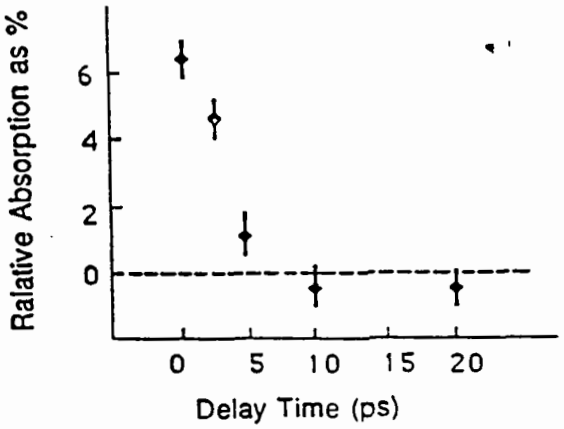

Figure 47. The dependence of bleaching, or saturation absorption, on delay time between pump and probe pulses in an eleven-layer polydiacetylene film.

VI. Conclusion

Nonlinear optical investigations of polymeric samples have revealed aspects of their electronic and conformational properties. The impact of attaching different functional groups onto the polymer chain may be assessed through measurements to ascertain the molecular hyperpolarizabilities, β and γ. In polymers possessing a conjugated π-electron system, the extent of electron delocalization can be inferred from the third order hyperpolarizability. Bulk properties, such as the degree of order in the sample, can be gauged from the macroscopic susceptibilities, $\chi^{(2)}$ and $\chi^{(3)}$. For example, a sample's ability to generate a second harmonic signal, which depends on $\chi^{(2)}$, is a direct indication of a non-centrosymmetric structure. The anisotropy of $\chi^{(3)}$ in polymeric systems, such as the polydiacetylenes, indicates the extent of order among the polymer chains.

The prospect of applications of nonlinear optics, in optical switching, data processing and frequency conversion, has partly driven

systems of polymers and organic molecules have been developed for their potential as electro-optical modulators. The optical properties of conjugated polymeric materials have been tested and scrutinized for their applicability in all-optical switching. Nonlinear spectroscopy has emerged as a essential tool in this effort to both characterize and optimize the nonlinear optical behavior of polymers for possible future applications.

Acknowledgement

The authors acknowledge partial support from the Office of Naval Research. Dianne Galotti provided conscientious and informed assistance throughout the preparation of this text. The manuscript was assembled in its final form through the cooperative efforts of Jeng-I Chen, Aloke Jain, Ru Jong Jeng, Lynne Samuelson, Xiao-Fang Sun and Kelli Zahn.

VII. References

1. J. Zyss, J. Mol. Electron., 1 (1985) 25-45.
2. G. T. Boyd, J. Opt. Soc. Am. B, 6 (1989) 685-692.
3. B. F. Levine and C. G. Bethea, J. Chem. Phys., 63 (1975) 2666-2682.
4. G. C. Baldwin, An Introduction to Nonlinear Optics, Plenum Press, New York, 1969, pp. 71-88, 99-104.
5. Y. R. Shen, The Principles of Nonlinear Optics, John Wiley & Sons, New York, 1984, pp. 86-107, 67-85, 108-116.
6. G. C. Baldwin, An Introduction to Nonlinear Optics, Plenum Press, New York, 1969, pp. 73-79, 88-97.
7. P. D. Maker and R. W. Terhune, Phys. Rev. A, 137 (1965) 801-818.
8. P. D. Maker, R. W. Terhune, M. Nisenoff and C. M. Savage, Phys. Rev. Lett., 8 (1962) 21-22.
9. S. K. Kurtz in H. Rabin and C. L. Tang, Quantum Electronics: A Treatise, Vol. 1., Nonlinear Optics, Part A, Academic Press, New York, 1975, pp. 263-281.
10. J. Jerphagnon and S. K. Kurtz, J. Appl. Phys., 41, (1970) 1667-1681.
11. Y. R. Shen, The Principles of Nonlinear Optics, John Wiley & Sons, New York, 1984, pp. 98-103.
12. J. C. Baumert, G. C. Bjorklund, D. H. Jundt, M. C. Jurich, H. Looser, R. D. Miller, J. Rabolt, R. Sooriyakumaran, J. D. Swalen and R. J. Twieg, Appl. Phys. Lett., 53 (1988) 1147-1149.
13. M. Thalhammer and A. Penzkofer, Appl. Phys. B, 32 (1983) 137-143.
14. J. Kerr, Phil. Mag., 50 (1875) 337-348,446-458.
15. F. C. A. Pockels, Neues Jahrb. Mineral., 7 (1891) 201-231; 8 (1893) 407-417.
16. G. Mayer and R. Gires, C. R. Acad. Sci., 258 (1963) 2039.
17. P. D. Maker, R. W. Terhune and C. W. Savage, Phys. Rev. Lett., 12 (1964) 507.

18. G. C. Baldwin, An Introduction to Nonlinear Optics, Plenum Press, New York, 1969, pp. 44-46, 109-111, 115-124.
19. Y. R. Shen, The Principles of Nonlinear Optics, John Wiley & Sons, New York, 1984, pp. 141-186.
20. M. D. Levenson, Introduction to Nonlinear Laser Spectroscopy, Academic Press, New York, 1982, pp. 17-21.
21. Y. R. Shen, The Principles of Nonlinear Optics, John Wiley & Sons, New York, 1984, pp. 267-275.
22. M. G. Albrecht and J. A. Creighton, J. Am. Chem. Soc., 99 (1977) 5215.
23. C. A. Murray in B. A. Garetz and J. Lombardi (Eds), Recent Advances in Laser Spectroscopy, Vol. 4, John Wiley and Sons, New York, 1975.
24. Y. R. Shen, The Principles of Nonlinear Optics, John Wiley & Sons, New York, 1984, pp. 242-275.
25. M. D. Levenson, Introduction to Nonlinear Laser Spectroscopy, Academic Press, New York, 1982, pp. 111.
26. Y. R. Shen, The Principles of Nonlinear Optics, John Wiley & Sons, New York, 1984, pp. 249-251.
27. F. E. Lytle, R. M. Parrish and W. T. Barnes, Appl. Spec., 39 (1985) 444-451.
28. P. A. Franken, A. E. Hill, C. W. Peters and G. Weinreich, Phys. Rev. Lett., 7 (1961) 118-119.
29. G. D. Boyd, R. C. Miller, K. Nassau, W. L. Bond and A. Savage, Appl. Phys. Lett., 5 (1964) 234.
30. R. C. Miller, G. D. Boyd and A. Savage, Appl. Phys. Lett., 6 (1965) 77-79.
31. A. Yariv, Quantum Electronics, Second Edition, John Wiley and Sons, New York, 1975, pp. 333, 416.
32. T. Y. Chang, Optical Engineering, 20 (1981) 220.
33. A. J. Heeger, J. Orenstein and D. R. Ulrich, Nonlinear Optical Properties of Polymers, MRS Symposium Proceedings, Pittsburgh, PA, Vol. 109, 1987.
34. J. G. Bergman, J. H. McFee and G. R. Crane, Appl. Phys. Lett., 18 (1971) 203.
35. S. J. Lalama and A. F. Garito, Phys. Rev. A, 20 (1979) 1179-1191.
36. A. F. Garito and K. D. Singer, Laser Focus, February (1982) 59-64.
37. T. Kaino, K. Kubodera, S. Tomaru, T. Kurihara, S. Saito, T. Tsutsui and S. Tokito, Electron. Lett., 23 (1987) 1095-1097.
38. T. Kaino, H. Kobayashi, K. Kubodera and T. Kurihara, Appl. Phys. Lett., 54 (1989) 1619-1621.
39. M. Sinclair, D. Moses, A. J. Heeger, K. Vilhelmsson, B. Valk and M. Salour, Solid State Commun., 61 (1987) 221-225.
40. A. Karpfen, J. Phys. C, 13 (1980) 5673-89.
41. C. Sauteret, J. P. Hermann, R. Frey, F. Pradere, J. Ducuing, R. H. Baughman and R. R. Chance, Phys. Rev. Lett., 36 (1976) 956-959.
42. G. P. Agrawal, C. Cojan and C. Flytzanis, Phys. Rev. D, 17 (1978) 776-789.
43. R. H. Baughman and R. R. Chance, J. Poly. Sci., Poly. Phys. Ed., 14 (1976) 2037-2045.
44. W. F. Lewis and D. N. Batchelder, Chem. Phys. Lett., 60 (1979) 232-237.
45. C. Flytzanis, C. Cojan and G. P. Agrawal, Nuovo Cimento, 39 (1977) 488-493.

G. Wegner, J. Pure & Appl. Chem., 49 (1977) 443-454.
R. J. Young in D. Bloor and R. R. Chance (Eds), Polydiacetylenes: Synthesis, Structure and Electronic Properties, Martinus Nijhoff Pub., Dordrecht, 1985, pp. 335-362.
48. M. Schott and G. Wegner in D. S. Chemla and J. Zyss (Eds), Nonlinear Optical Properties of Organic Molecules and Crystals, Vol. 2, Academic Press, Orlando, 1987, pp. 3-49.
49. J. F. Nicoud and R. J. Twieg in D. S. Chemla and J. Zyss (Eds), Nonlinear Optical Properties of Organic Molecules and Crystals, Vol. 1, Academic Press, Orlando, 1987, pp. 227-296.
50. M. J. S. Dewar, J. Chem. Soc. (1950) 2329-2334.
51. B. J. Orchard and S. K. Tripathy, Macromolecules, 19 (1986) 1844.
52. H. Nakanishi, H. Matsuda, M. Kato, K. Okuhara and A. Ueda, Polym. Preprint Japan, 33 (1984) 668.
53. S. S. Kumar, R. S. Kumar, L. A. Samuelson, J. Kumar, A. Blumstein, and S. K. Tripathy, Proceedings of the Fourth International Conference on Langmuir-Blodgett Films, Tsukuba, Japan, April 24-29, 1989 to be published in Thin Solid Films.
54. M. Thakur and S. Meyler, Macromolecules, 18 (1985) 2341-2344.
55. G. M. Carter, M. K. Thakur, Y. J. Chen and J. V. Hryniewicz, Appl. Phys. Lett., 47 (1985) 457-459.
56. D. J. Williams in D. S. Chemla and J. Zyss (Eds), Nonlinear Optical Properties of Organic Molecules and Crystals, Vol. 1, Academic Press, Orlando, 1987, pp. 405-435.
57. D. J. Williams, Agnew. Chem. Int. Ed. Engl., 23 (1984) 690-703.
58. J. R. Hill, P. L. Dunn, G. J. Davies, S. N. Oliver, P. Pantelis and J. D. Rush, Electron. Lett., 23 (1987) 700-701.
59. P. Pantelis, J. R. Hill and G. J. Davies, Abs. Pap. ACS, 193(Apr.) (1987) 183.
60. K. D. Singer, S. L. Lalama, J. E. Sohn and R. D. Small in D. S. Chemla and J. Zyss (Eds), Nonlinear Optical Properties of Organic Molecules and Crystals, Vol. 1, Academic Press, Orlando, 1987, pp. 437-468.
61. V. K. Agrawal, Phys. Today, June (1988) 40-46.
62. D. R. Day and J. B. Lando, Macromolecules, 13 (1980) 1483.
63. M. Pomerantz and A. Segmuller, Thin Solid Films, 68 (1980) 33-45.
64. J. D. Swalen, J. Mol. Electron., 2 (1986) 155-181.
65. L. M. Blinov, Russ. Chem. Rev., 52 (1983) 713-735.
66. A. Barraud and M. Vandevyver in D. S. Chemla and J. Zyss (Eds), Nonlinear Optical Properties of Organic Molecules and Crystals, Vol. 1, Academic Press, Orlando, 1987, pp. 357-383.
67. J. F. Rabolt, R. Santo, N. E. Schlotter and J. D. Swalen, IBM J. Res. Develop., 26 (1982) pp. 209-216.
68. S. T. Kowel, L. Ye, Y. Zhang, L. M. Hayden, Opt. Eng., 26 (1987) 107-112.
69. L. Sebastian and G. Weiser, Phys. Rev. Lett., 46 (1981) 1156-1159.
70. L. Sebastian and G. Weiser, Chem. Phys., 62 (1981) 447-457.

G. Weiser and L. Sebastian in D. Bloor and R. R. Chance, (Eds), Polydiacetylenes: Synthesis, Structure and Electronic Properties, Martinus Nijhoff Pub., Dordrecht, 1985, pp. 213-222.
72. K. Lochner, H. Bassler, B. Tieke and G. Wegner, Phys. Stat. Sol. (b), 88 (1978) 653.
73. Y. Tokura, T. Koda, A. Itsubo, M. Miyabayashi, K. Okuhara and A. Ueda, J. Chem. Phys., 85 (1986) 99-104.
74. Y. Tokura, Y. Oowaki, Y. Kaneko, T. Koda and T. Mitani, J. Phys. Soc. Jpn., 53 (1984) 4054-4063.
75. Y. Tokura, Y. Oowaki, T. Koda and R. H. Baughman, Chem. Phys., 88 (1984) 437-442.
76. R. Worland, S. D. Philips, W. C. Walker and A. J. Heeger, Synthetic Metals, 28 (1989) D663-D667.
77. C. C. Teng and A. F. Garito, Phys Rev. Lett., 50 (1983) 350-352.
78. C. C. Teng and A. F. Garito, Phys Rev. B, 28 (1983) 6766-6773.
79. B. F. Levine and C. G. Bethea, J. Chem. Phys., 65 (1976) 1989-1993.
80. G. Berkovic and Y. R. Shen, in P. N. Prasad and D. R. Ulrich (Eds.), Nonlinear Optical and Electroactive Polymers, Plenum Press, New York, 1988, pp. 157-168.
81. I. R. Girling, N. A. Cade, P. V. Kolinsky, R. J. Jones, I. R. Peterson, M. M. Ahmad, D. B. Neal, M. C. Petty, G. C. Roberts and W. J. Feast, J. Opt. Soc. Am. B, 4 (1987) 950-954.
82. O. A. Aktsipetrov, N. N. Akhmediev, E. D. Mishina and V. R. Novak, JETP Lett., 37 (1983) 207-209.
83. G. Marowsky, A. Gierulski, R. Steinhoff, D. Dorsch, R. Eidenschnik and B. Riefer, J. Opt. Soc. Am. B, 4 (1987) 956-961.
84. I. R. Girling, N. A. Cade, P. V. Kolinsky, J. D. Earls, G. H. Cross and I. R. Peterson, Thin Solid Films, 132 (1985) 101-112.
85. I. R. Girling, N. A. Cade, P. V. Kolinsky, and C. M. Montgomery, Elect. Lett., 21 (1985) 169-170.
86. I. R. Girling, P. V. Kolinsky, N. A. Cade, J. D. Earls, and I. R. Peterson, Opt. Comm., 55 (1985) 289-292.
87. P. A. Chollet, F. Kajzar and J. Messier, Thin Solid Films, 132 (1985) 1-10.
88. L. M. Hayden, S. T. Kowel and M. P. Srinivasan, Opt. Comm., 61 (1987) 351-356.
89. S. T. Kowel, L. M. Hayden and R. H. Selfridge, SPIE Proceedings, 682 (1986) 103-108.
90. P. Stroeve, M. P. Srinivasan, B. G. Higgins and S. T. Kowel, Thin Solid Films, 146 (1987) 209-220.
91. L. M. Hayden, B. L. Anderson, J. Y. S. Lam, B. G. Higgins, P. Stroeve and S. T. Kowel, Thin Solid Films, 160 (1988) 379-388.
92. G. Berkovic, R. Superfine, P. Guyot-Sionnest, Y. R. Shen, and P. N. Prasad, J. Opt. Soc. Am. B, 5 (1988) 668-673.
93. P. A. Chollet, F. Kajzar, J. Messier, in D. Bloor and R. R. Chance (Eds.), Polydiacetylenes: Synthesis, Structure and Electronic Properties, Martinus Nijhoff Pub., Dordrecht, 1985, pp. 317-324.

H. Sato, T. Yamamoto, I. Seo and H. Gamo, Opt. Lett., 12 (1987) 579.
P. Robin, E. Chastaing, D. Broussoux, J. Raffy, J. P. Pocholle, Proceedings of Conference on Lasers and Electro-optics, Baltimore, Maryland, U.S.A., April 24 - 28, 1989, Optical Society of America, Washington, DC, 1989, pp. 74.
96. G. R. Meredith, J. G. VanDusen and D. J. Williams, Macromolecules, 15 (1982) 1385-1389.
97. K. D. Singer, M. G. Kuzyk and J. E. Sohn, in P. N. Prasad and D. R. Ulrich (Eds.), Nonlinear Optical and Electroactive Polymers, Plenum Press, New York, 1988, pp. 189-204.
98. K. D. Singer, M. G. Kuzyk and J. E. Sohn, J. Opt. Soc. Am. B, 4 (1987) 968-976.
99. K. D. Singer, J. E. Sohn and S. J. Lalama, Appl. Phys. Lett., 49 (1986) 248-250.
100. K. D. Singer, S. J. Lalama and J. E. Sohn, SPIE Proceedings, 578 (1985) 130-136.
101. M. G. Kuzyk, K. D. Singer, H. E. Zahn and L. A. King, J. Opt. Soc. Am. B, 6 (1989) 742-752.
102. H. L. Hampsch, J. Yang, G. K. Wong and J. M. Torkelson, Macromolecules, 21 (1988) 528-530.
103. C. Ye, T. J. Marks, J. Yang and G. K. Wong, Macromolecules, 30 (1987) 2322-2324.
104. M. A. Mortazavi, A. Knoesen, S. T. Kowel, B. G. Higgins and A. Dienes, J. Opt. Soc. Am. B, 6 (1989) 733-741.
105. G. R. Meredith, B. Buchalter, and C. Hanslik, J. Chem. Phys., 78 (1983) 1533.
106. F. Kajzar and J. Messier, Phys. Rev. A, 32 (1985) 2352.
107. F. Kajzar, J. Messier, J. Zyss and I. Ledoux, Opt. Comm., 45 (1983) 133-137.
108. F. Kajzar, J. Messier and J. Zyss, J. Physique, 44 (1983) C3-709-C3-712.
109. F. Kajzar and J. Messier, Thin Solid Films, 132 (1986) 11-19.
110. F. Kajzar and J. Messier in D. S. Chemla and J. Zyss (Eds.), Nonlinear Optical Properties of Organic Molecules and Crystals, Vol. 2, Academic Press, Orlando, 1987, pp. 51-83.
111. F. Kajzar, J. Messier and C. Rosilio, J. Appl. Phys., 60 (1986) 3040-3044.
112. F. Kajzar and J. Messier, J. Opt. Soc. Am B, 4 (1987) 1040-1046.
113. D. M. Gookin and J. C. Hicks in S. Musikant (Ed.), Advances in Materials for Active Optics, SPIE Proceedings, 567 (1985) 41-43.
114. F. Kajzar, S. Etemad, G. L. Baker and J. Messier, Synth. Metals, 17 (1987) 563-567.
115. G. Berkovic, Y. R. Shen and P. N. Prasad, J. Chem. Phys., 87 (1987) 1897-1898.
116. S. Matsumoto, K. Kubodera, T. Kurihara and T. Kaino, Appl. Phys. Lett., 51 (1987) 1.
117. G. M. Carter, Y. J. Chen and S. K. Tripathy, Appl. Phys. Lett., 43 (1983) 891-893.
118. P. P. Ho, N. L. Yang, T. Jimbo, Q. Z. Wang and R. R. Alfano, J. Opt. Soc. Am. B, 4 (1987) 1025-1029.
119. P. P. Ho, R. Dorsinville, N. L. Yang, G. Odian, G. Eichmann, T. Jimbo, Q. Z. Wang, G. C. Tang, N. D. Chen, W. K. Zou, Y. Li and R. R. Alfano, SPIE Proceedings, 682 (1986) 36-43.

H. Sixl and R. Warta in X. Kuzmany, M. Mehring and E. Roth (Eds.), Electronic Properties of Polymers, Springer-Verlag, New York, 1985, pp. 246-248.
. D. Bloor, S. D. D. V. Rughooputh, D. Phillips, W. Hayes and K. S. Wong in H. Kuzmany, M. Mehring and E. Roth (Eds.), Electronic Properties of Polymers, Springer-Verlag, New York, 1985, pp. 253-255.
122. H. Uchiki and T. Kobayashi, J. Appl. Phys., 64 (1988) 2625-2629.
123. M. G. Kuzyk and C. W. Dirk, Appl. Phys. Lett., 54 (1989)1628-1630.
124. K. D. Singer, M. G. Kuzyk, W. R. Holland, J. E. Sohn, S. J. Lalama, R. B. Comizzoli, H. E. Katz and M. L. Schilling, Appl. Phys. Lett., 53 (1988) 1800-1802.
125. B. I. Greene, M. Thakur and J. Orenstein, Appl. Phys. Lett., 54 (1989) 2065-2067.
126. Y. J. Chen, G. M. Carter and S. K. Tripathy, Solid State Communication, 54 (1985) 19.
127. G. M. Carter, Y. J. Chen, M. F. Rubner, D. J. Sandman, M. K. Thakur and S. K. Tripathy, in D. S. Chemla and J. Zyss (Eds), Nonlinear Optical Properties of Organic Molecules and Crystals, Vol. 2, Academic Press, Orlando, 1987, 85-120.
128. R. Burzynski, P. N. Prasad, J. Biegajski and D. A. Cadenhead, Macromolecules, 19 (1986) 1059-1062.
129. M. L. Shand and R. R. Chance in D. J. Williams (Ed) Nonlinear Optical Properties of Organic and Polymeric Materials, American Chemical Society, Washington DC, 1983, pp. 187-212.
130. R. R. Chance, M. L. Shand, C. Hogg and R. Silbey, Phys. Rev. B, 22 (1980) 3540-3550.
131. W. M. Hetherington III, N. E. Van Wyck, E. W. Koenig, G. I. Stegeman and R. M. Fortenberry, Opt. Lett., 9 (1984) 88-89.
132. J. Swiatkiewicz, X. Mi, P. Chopra and P. N. Prasad, J. Chem. Phys., 87 (1987) 1882-1886.
133. P. N. Prasad, Thin Solid Films, 152 (1987) 275-294.
134. D. N. Rao, J. Swiatkiewicz, P. Chopra, S. K. Ghoshal and P. N. Prasad, App. Phys. Lett., 48 (1986) 1187-1189.
135. G. M. Carter, J. Opt. Soc. Am. B, 4 (1987) 1018-1024.
136. G. M. Carter, J. V. Hryniewicz, M. K. Thakur, Y. J. Chen and S. E. Meyler, Appl. Phys. Lett., 49 (1986) 998-1000.
137. W. M. Dennis, W. Blau and D. J. Bradley, Appl. Phys. Lett., 47 (2985) 200.
138. D. N. Rao, P. Chopra, S. K. Ghoshal, J. Swiatkiewicz and P. N. Prasad, J. Chem. Phys., 84 (1986) 7049.
139. T. Hattori and T. Kobayashi, Chem. Phys. Lett., 133 (1987) 110-114.
140. Y. Wang and W. Mahler, Opt. Comm., 61 (1987) 233-236.
141. Maloney and W. Blau, J. Opt. Soc. Am. B, 4 (1987) 1035-1039.
142. H. Fujiwara and K. Nakagawa, Opt. Comm., 66 (1988) 307-310.
143. L. Yang, R. Dorsinville, Q. Z. Wang, W. K. Zou, P. P. Ho, N. L. Yang, R. R. Alfano, R. Zamboni, R. Danieli, G. Ruani and C. Taliani, J. Opt. Soc. Am. B, (1989) 753-756.
144. L. Yang, Q. Z. Wang, P. P. Ho, R. Dorsinville, R. R. Alfano, W. K. Zou and N. L. Yang, Appl. Phys. Lett., 53 (1988) 1245-1247.
145. D. J. McGraw and A. E. Siegman, Appl. Phys. Lett., 54 (1989) 1713-1715.
146. M. T. Zhao, B. P. Singh and P. N. Prasad, J. Chem. Phys., 89 (1988) 5535-5541.
147. P. Cong, Y. Pang and P. N. Prasad, J. Chem. Phys. 85 (1986) 1077.

148. K. C. Lim, A. Kapitulnik, R. Zacher and A. J. Heeger, J. Chem Phys., 82 (1985) 516-521.
149. K. C. Lim and A. J. Heeger, J. Chem. Phys., 82 (1985) 522-530.
150. T. Kobayashi, H. Ohtani and K. Kurokawa, Chem. Phys. Lett., 121 (1985) 356-360.
151. T. Kobayashi and H. Ikeda, Chem. Phys. Lett., 133 (1987) 54-58.
152. T. Kobayashi and H. Ikeda, Synth. Metals, 18 (1987) 441-446.
153. T. Kobayashi, J. Iwai and M. Yoshizawa, Chem. Phys. Lett., 112 (1984) 360-364.
154. B. I. Greene, J. Orenstein, R. R. Millard and L. R. Williams, Phys. Rev. Lett., 58 (1987) 2750-2753.
155. S. Schmitt Rink, D. S. Chemla and D. A. B. Miller, Phys. Rev. B, 32 (1985) 6601.
156. B. I. Greene, J. Orenstein, R. R. Millard and L. R. Williams, Chem. Phys. Lett., 139 (1987) 381-385.
157. B. I. Greene, J. F. Mueller, J. Orenstein, D. H. Rapkine, S. Schmitt-Rink and M. Thakur, Phys. Rev. Lett., 61 (1988) 325-328.
158. A. Mysyrowicz, D. Hulin, A. Antonetti, A. Migus, W. T. Masselink and H. Morkoc, Phys. Rev. Lett., 56 (1986) 2748-2751.
159. T. Kobayashi, U. Stamm, M. Taiji, M. Yoshizawa, K. Yoshino, CLEO '89 Conference on Lasers and Electro-Optics, April 28, 1989, FHH3.
160. J. P. Heritage, G. J. Blanchard, A. von Lehmen, G. L. Baker, S. Etemad, CLEO '89 Conference on Lasers and Electro-Optics, April 28, 1989, FHH2.
161. F. Kajzar, L. Rothberg, S. Etemad, P. A. Chollet, D. Grec, A. Boudet and T. Jedju, Opt. Comm., 66 (1988) 55-58.